Università degli Studi di Napoli "Federico II"

SCUOLA POLITECNICA E DELLE SCIENZE DI BASE

DIPARTIMENTO DI INGEGNERIA INDUSTRIALE

CORSO DI LAUREA IN INGEGNERIA AEROSPAZIALE

CLASSE DELLE LAUREE IN INGEGNERIA INDUSTRIALE (L-9)

BACHELOR THESIS

PRELIMINARY SIZING AND AERODYNAMICS OF AN ELECTRIC POWERED RC AIRCRAFT

SUPERVISOR:

Dr. DANILO CILIBERTI

CO-SUPERVISOR:

Prof. Eng. FABRIZIO NICOLOSI

CANDIDATE:

MARCO MAZIO

Matricola: N35002674

ANNO ACCADEMICO 2019/2020

Index

List of figures

List of tables

~ La curiosità è alla base della conoscenza ~

Chapter 1
Introduction

1. Team Organization

The team appointed to the realization of the model is a subgroup of the team formed in 2019 to participate in the Design Build and Fly (DBF) competition that would have been held the following year. The missions and requirements taken into consideration have been established starting from the ones of the competition. This project has given to each member of the team the opportunity to improve several soft skills such as team working and problem solving which are relevant and decisive for an engineer. In addition, this experience has allowed to deepen knowledge in the Aerospace Engineering field, providing the fundamentals of aircraft design in the context of an experimental bachelor's thesis.

The team counts five members to better focus each one's work on the five branches identified that will lead to the final design of the aircraft, called by the team as "UninAir". Consequently, every member of the team is the leader of their own branch and therefore its manager. The team has been supervised by two advisors that proved guidance to the team throughout the whole project. The identified branches concern: the study of the aerodynamics of the aircraft through the use of software such as AIRFOIL and XFLR5; examination of the stability of the model with the aid of the program created by NASA, OpenVSP; structural analysis, in particular an accurate check was performed on the wing structure, in presence of aerodynamic loads; aircraft performance analysis (polar curves, propeller performance). It is clear that each branch is not isolated from the others, but there is a strong link between all the application fields considered and therefore a coordinated work by each member of the Team is required.

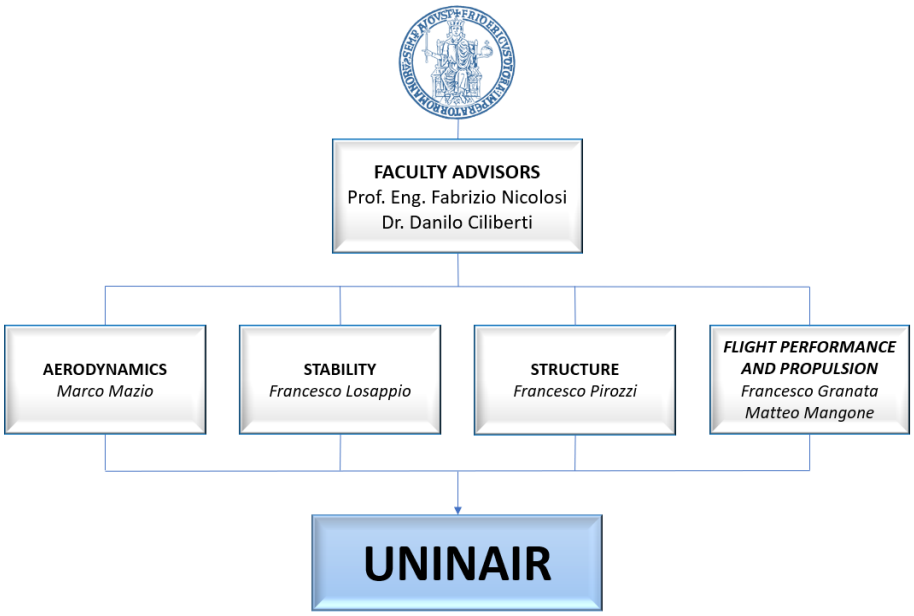

Figure 1.1 - Team Organization

1.1 Requirements

The main purpose of the team was to carry as many passengers as possible in order to allow the aircraft to conduct charter flights recovering expenses. In the table below, there is an overview of the requirements that the team had to respect during the project:

Table 1.1 - Requirements

Maximum allowable wingspan	$5\ ft = 1{,}5\ m$
Take-Off Gross Weight with payload	$TOGW < 55\ lb = 25\ kg$
Passenger Weight	$5\ oz = 113{,}4\ g$
Luggage Weight	$1\ oz = 28{,}35\ g$
Take-Off Run	$23\ ft = 7\ m$
Ground for the take-off	$Dirt$
Endurance	$10\ min$
Minimum load for bending test	$\pm\ 3x\ MTOW$
Type of Propulsion	$Electric$

In addition, the aircraft has to follow the path shown in the figure, and each lap must be completed in 2 minutes in order for passengers to have a comfortable and safe flight.

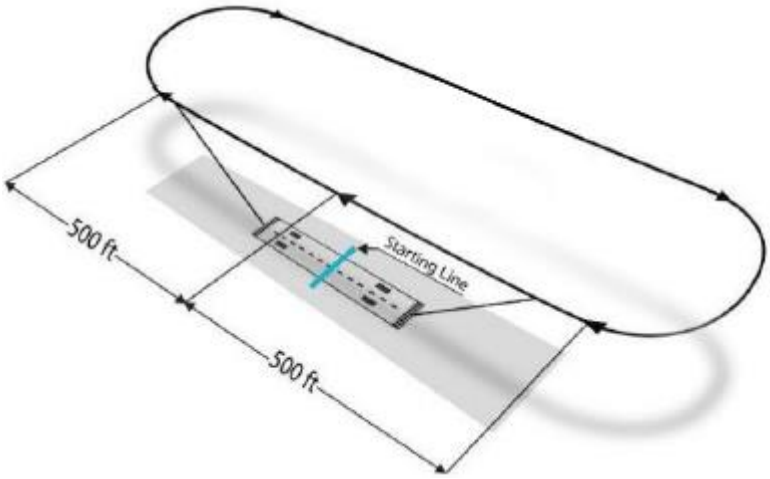

Figure 1.2 - Competition Flight Course

The dimension of each passenger and luggage are defined as it is showed below:

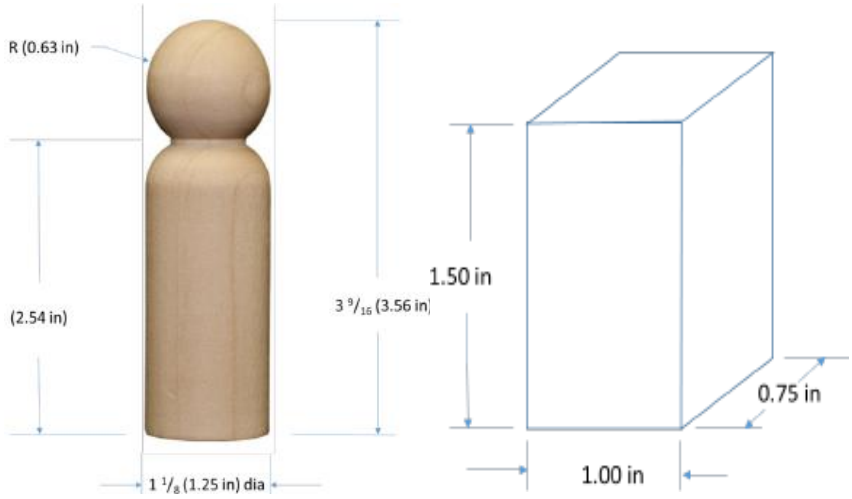

Figure 1.3 - Passenger and Luggage

Chapter 2

Preliminary Design and Sizing

2. Design Selection Process

In order to properly choose the best configuration for the aircraft, the team has compiled a table of merit based on the most important configuration factors. It has been assigned a score from 0 to 5 for each one, depending on the mission requirements.

Table 2.2 - Table of merit

Factor	Importance
Structural Weight	4
Maneuverability	3
Passengers Capability	5
Speed	3,5
Manufacturability	4,5
Take-OFF Run	2,5
Reliability	2,5

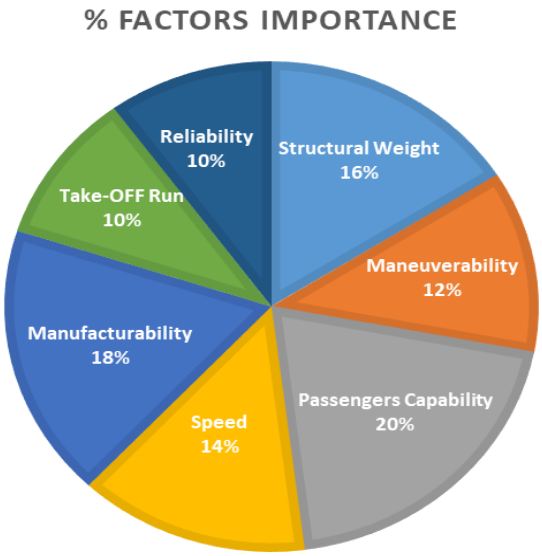

- **Structural Weight**: the weight strongly influences the performance of the aircraft, indeed a lower structural weight means whether less consumption or more payload transportable.
- **Maneuverability**: the capability to safely control the aircraft as well as its stability and fast maneuvers are also important to complete all the laps on time.
- **Passengers Capability**: this is the most important factor because carrying as many passengers as possible would provide more income for the charter company.
- **Speed**: the airplane speed contributes to complete faster the mission, although a trade-off study is necessary to avoid an excessive consumption of the batteries.
- **Manufacturability**: the ease of manufacturing is essential for building the aircraft by the team itself. Therefore, some configurations have been rejected due to tricky manufacturing and lack of solid executive experience alike.

- **Take-Off Run**: having a short take-off run is included among the requirements. This forced the team to take into account configurations that would provide advantages on those terms.
- **Reliability**: to guarantee the safety during the missions (take-off, cruise and landing), the reliablitiy of the aircraft is not a negligible factor.

Table 2.3 - Final Design Decision

Feature	Configuration	Wing	Tailplane	Engine	Landing Gear	Fuselage
Result	CONVENTIONAL	LOW	CONVENTIONAL	SINGLE/TWIN	TRICYCLE	RECTANGULAR

The final conceptual design has been chosen by analyzing the total score gained by each different configuration in terms of Structural Weight, Maneuverability, Passenger Capability, Speed, Manufacturability, Take-off Run and Reliability as shown so far. The total score is obtained by adding up scores assigned to each possible configuration as it will be shown further into this document.

2.1 Conceptual Design

Considering the requirements of the mission, it is appropriate to present the layout of the team's arguments regarding how the bulk of the design was figured out. As a general note, the focus was on:

- Main wing configuration
- Main wing positioning
- Tail section
- Engines
- Landing gear
- Fuselage

This preliminary discussion is crucial in order to further analyze the capabilities of the aircraft. The choice made on those regards will form the foundations of the specialized studies that aim to reach the optimal configuration.

Table 2.4 - Design Alternatives

Component	Alternatives		
Wing Layout	Conventional	Biplane	Flying Wing
Wing Positioning	Low	High	
Empennage Type	V-Tail	Conventional	T-Tail
Number of Engines	1	2	
Landing Gear	Taildragger	Tricycle	
Fuselage section	Smoothed Rectangular	Circular	

2.1.1 Main Wing Configuration

The choice of the main wing configuration of the aircraft is the first aspect on which attention has been focused upon. That is because it is important to adapt the subsequent decisions regarding the individual components of the aircraft to this primary one.
The considered configurations are:

- CONVENTIONAL: it is composed by the tail plane (horizontal and vertical) and one main wing.
- BIPLANE: two overlapping wings which are parallel to each other although they may have different shapes and sizes.
- FLYING WING: flying wing aircraft without fuselage and tail plane.

By a structural weight's point of view, the best one is the flying wing since it is the lightest, because of the tail plane absence. However, the flying wing does not excel on directional stability due to the absence of the fin and this directly affects manoeuvrability. It is important to point out that the flying wing configuration will have a high longitudinal stability if equipped with reflex airfoil (self-stable) and if the warping factors and the sweep angle are well evaluated.

Regarding the biplane, it must be said that with the same wingspan of a conventional configuration there is twice as much wing area, halving the wing load. Moreover, the eventual presence of a double aileron implies a higher roll rate and therefore more lateral manoeuvrability.

Focusing on reliability, the conventional configuration is the best known of the three considered and therefore well proven to be dependable. The biplane is frequently subject to assembly inaccuracies since it is the most complex.

Both the biplane and flying wing models are very difficult to manufacture because they require unconventional construction techniques. On the other hand, the conventional configuration is the simplest to manufacture.

The flying wing is the one that generates less drag among the three. On the other hand, the biplane configuration, with the presence of two main lift generators, create four vortex that massively increases aerodynamic drag. The conventional is a good compromise between the previous two.

Regarding the passenger's capacity, the biplane is the most inconvenient because it is difficult to create a passage for the insertion of passengers due to the presence of wing braces between the two wings.

Biplane configuration has a lower take off length since, with the same wingspan, the wing surface is two times bigger and therefore the wing load decreases. The opposite situation occurs with the flying wing, also because of the lack of flaps.

Table 2.5 - Configuration Trade Study

CONFIGURATION TRADE STUDY							
		CONVENTIONAL		FLYING WING		BIPLANE	
Attribute	Weighting	Insert Score	Weighted Score	Insert Score	Weighted Score	Insert Score	Weighted Score
Structural Weight	16%	0.6	0.096	1	0.16	0.3	0.048
Manoeuvrability	12%	0.8	0.096	0.5	0.06	0.6	0.039
Passengers Capability	20%	0.8	0.16	0.3	0.06	0.7	0.081
Speed	14%	0.8	0.112	1	0.14	0.4	0.037
Manufacturability	18%	1	0.18	0.25	0.045	0.5	0.065
Take-Off Run	10%	0.9	0.09	0.7	0.07	1	0.083
Reliability	10%	1	0.1	0.5	0.05	0.6	0.055
Totals	100%		0.83		0.59		0.41

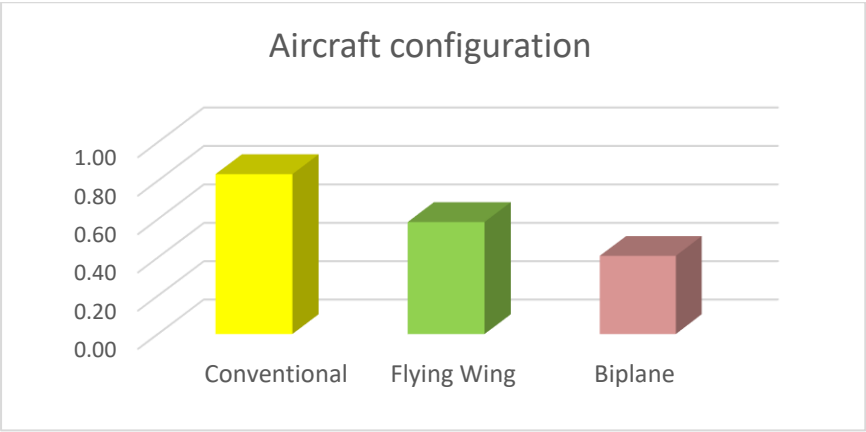

Figure 2.4 - Configuration Trade Study

2.1.2 Wing Positioning

Once opted for the conventional configuration for our aircraft, two different wing positions have been taken into consideration: high wing and low wing. As it is showed in the table below, the passenger capability is the parameter which most influenced our choice.

In terms of structural weight, the low wing configuration is slightly better because it allows to embed the spar in the force frames. This is not possible with a high wing that should be installed on the upper surface of the fuselage. However, in case of braced wing, the root sections could be slenderer because in that zone the momentum is null.

An aircraft with high wing has a better (static) lateral stability thanks to the dihedral effect (which gives a negative injection to the coefficient $C_{\mathcal{L}_\beta}$). Indeed, as shown in the figure below, a side wind (i.e. sideslip) causes an overpressure under the upwind wing and therefore the aircraft tends to stabilize thanks to the rolling moment generated. On the other hand, low wings provide better aerodynamic performance due to the absence of the joints between wing and fuselage that is less interference drag. Moreover, it might help to reduce the take-off run taking advantage of the ground effect.

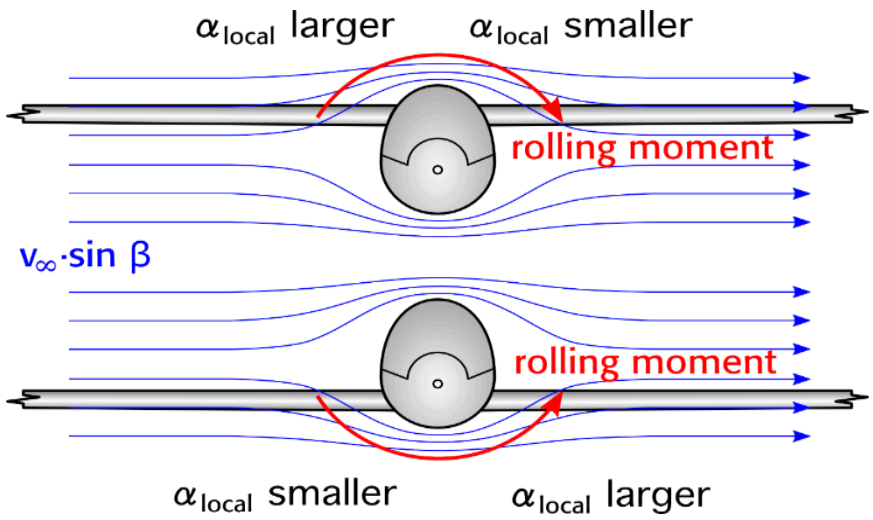

Figure 2.5 - Rolling Moment

As regards reliability, in case of imprecise landing, the high wing configuration is safer because the clearance is greater than it is with the low wing one which, instead, may impact on the ground if the airplane is banked.

The most important feature of the low wing configuration is that it guarantees a straightforward building and a simple access to the compartment where the passengers and luggage are stored. In addition, this configuration makes the assembly of the wing easier or its substitution alike. On the contrary, with a high wing, the loading and unloading of payload is likely to be trickier.

Table 2.6 - Wing Configuration Trade Study

WING CONFIGURATION TRADE STUDY					
		HIGH		LOW	
Attribute	Weighting	Insert Score	Weighted Score	Insert Score	Weighted Score
Structural Weight	16%	0.4	0.064	1	0.16
Manoeuvrability	12%	0.6	0.072	0.8	0.096
Passengers Capability	20%	0.5	0.1	1	0.2
Speed	14%	0.4	0.056	0.7	0.098
Manufacturability	18%	0.6	0.108	0.9	0.162
Take-Off Run	10%	0.5	0.05	0.8	0.08
Reliability	10%	0.9	0.09	0.4	0.04
Totals	100%		0.54		0.836

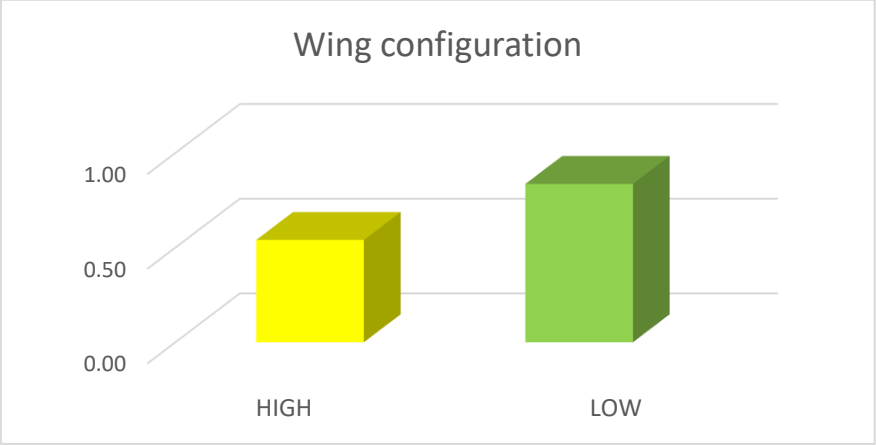

Figure 2.6 - Wing Configuration Trade Study

2.1.3 Tail

Once the configuration of the main wing is established, it is fundamental to discuss characteristics of the tail plane, specifically on a matter of stability, controllability, and reliability.

The main types of tail planes currently adopted by the aerospace industry are: conventional, T-tails, and V-tails. All of those options provide the aircraft with specific advantages and drawbacks that require a careful analysis.

It seems clear that the weight of the structure that support the aerodynamic surfaces of the tail plane will not be a major point of this discussion since it contributes only by a little percentage (estimated 5%) of the total inertial forces of the model aircraft.

The key point to analyse is instead how a different configuration plays into the overall stability and control of the aircraft, underlining the effect that each one has on the take-off distance.

The T-tail is composed by a vertical stabilizer which holds, within itself, the support structure of the horizontal stabilizer, placed at its tip. This particular kind of tail plane offers the advantage of working in an undisturbed airflow, allowing it to generate more lift at lower speed. Indeed, the dynamic pressure hitting the horizontal plane is unaffected by the downwash of the main wing, bringing the $\eta_H \cong 1$. At the same time, the horizontal tail reduces the magnitude of the vertical tail tip vortex, increasing the vertical tail effectiveness in sideslip, a phenomenon called end-plate effect.

Many times these advantages are outshined by a safety flaw of the T configuration. On extreme stall condition, the cone of turbulent flow coming from the main wing might engulf the tail plane, reducing its power of control turning it not effective altogether. This reason, along with an increased load on the vertical stabilizer, brought the team to reject the T-tail configuration.

T-tail is also prone to flutter, a dynamic aeroelastic phenomenon that must be avoided to fly safely. Tail flutter can rapidly destroy the empennage, leaving the aircraft without stability and control. To avoid flutter, the T-tail must have a very strong and rigid structure, which will increase the structural weight, opposing its aerodynamic advantage.

In contrast with all standard configurations, the V-tail consists in only two aerodynamic surfaces, they are tilted at an angle and often fixed on the upper side of the aircraft, effectively getting rid of one of the three wings that form the usual tail plane design. This of course makes the tail lighter, but, as we previously discussed, that is not an important issue for the analysis. Once again, the focus is on the ability of this configuration to provide stability and control authority during flight. The main feature of the V-tail is that the control power of rudder and equalizer is mixed and enforced using only two control surfaces. Yaw and pitch are consequently less effective unless the dimensions of the tail increase. This potential lack of power of the mixed equalizer might also result into a less performant take-off, that is one of the given requirements for the aircraft.

Therefore, the attention was focused on the conventional design for the tail plane. Both the deeper understanding for its properties and the possibility of installing a stabilator (since the stabilator is fitted into the fuselage) give this design an edge over the other two.

Table 2.7 - Tail Configuration Trade Study

TAIL CONFIGURATION TRADE STUDY							
		T		CONVENTIONAL		V	
Attribute	Weighting	Insert Score	Weighted Score	Insert Score	Weighted Score	Insert Score	Weighted Score
Structural Weight	16%	0.7	0.112	1	0.16	0.5	0.08
Manoeuvrability	12%	1	0.120	1	0.120	0.2	0.024
Passengers Capability	20%	0	0	0	0	0	0
Speed	14%	0.8	0.112	1	0.140	1	0.140
Manufacturability	18%	0.75	0.135	1	0.180	0.1	0.018
Take-Off Run	10%	1	0.100	1	0.100	0.25	0.025
Reliability	10%	0.7	0.070	1	0.100	0.2	0.020
Totals	100%		0.65		0.80		0.31

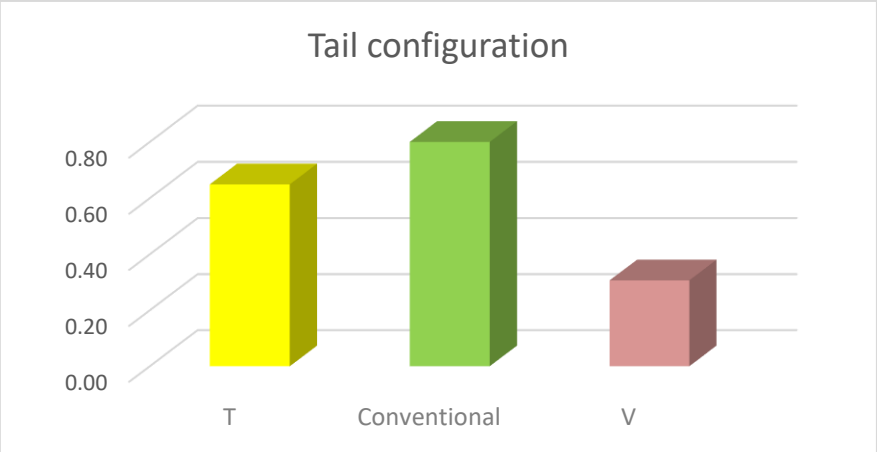

Figure 2.7 - Tail Configuration Trade Study

2.1.4 Number of Engines

Several factors were taken into account while conducting the propulsion system trade study for the aircraft. In particular, the aim of this subparagraph is to understand what the best number of engines is to install on the aircraft and therefore choose the single-engine configuration or the twin-engine configuration.

Firstly, a single engine configuration shall guarantee a certain overall weight saving since the battery pack should be lighter than the one needed for two engines. On the other hand, while a single engine would be installed on the aircraft's nose, in case of the twin-engine configuration, the engines would be installed on the wing structure. The presence of two inertial masses on the wing would make the total wing load decrease, thus the wing itself would be less stressed during flight. However, if the engines are installed on the wing, then a strengthened structure is needed where the engines are attached to the wing. That might mitigate the weight advantages aforementioned and would undermine the ease of manufacturing of the wing. Moreover, the CG of the wing sections that are behind the engine might shift ahead of the aerodynamic centre. This might increase the torque insisting on the wing structure.

The position of the engines also influences the manoeuvrability and stability of the aircraft. If the engine is on the aircraft's nose then it will not be influenced by the upwash generated by the wing, therefore the phenomena of non-axial flow, derived by the interaction air-wing, can be ignored. Furthermore, the energised flow behind the propeller increases the efficiency of the aerodynamic surfaces both of the horizontal tail plane and, in a lesser extent, the main wing. However, a twin-engine configuration ensures a better lateral control as it is possible to realise a differential thrust in order to help the rudder in case of need. At the same time, two engines require a bigger and strengthened rudder because it must guarantee directional controllability in case of one inoperative engine (OEI). It has to be said that in the unlucky event of a double engine failure, the presence of two propellers would induce more drag on the gliding aircraft than in case of one engine.

Moreover, two engines installed on the wing might be an obstacle while loading and unloading passengers as they would be close to the fuselage part that needs to be open during ground operations. Thus, for this reason and to guarantee a certain clearance from the ground, the propellers' diameter might need to be too limited. While it is true that in case of OEI condition a twin-engine configuration doesn't force the aircraft to abort the mission it is meant to accomplish, it also requires a more complicated electrical system and one more channel on the aircraft's controller than the single-engine configuration. Two engines also imply more maintenance and greater difficulty in case of substitution or repair of one of the engines.

In fact, it is not possible to decide without more specific considerations which configuration to choose. Therefore, once the aircraft geometry and structural characteristics will be more or less fixed, both studies about the single-engine and the twin-engine configuration will be further conducted to have a better understanding of the problem.

Table 2.8 - Engine Configuration Trade Study

ENGINE CONFIGURATION TRADE STUDY					
		SINGLE		TWIN	
Attribute	Weighting	Insert Score	Weighted Score	Insert Score	Weighted Score
Structural Weight	16%	1	0.16	0.5	0.08
Manoeuvrability	12%	1	0.120	0.3	0.036
Passengers Capability	20%	0.6	0.120	1	0.200
Speed	14%	0.5	0.070	1	0.140
Manufacturability	18%	1	0.180	0.75	0.135
Take-Off Run	10%	0.7	0.070	1	0.100
Reliability	10%	0.5	0.050	1	0.100
Totals	100%		0.77		0.79

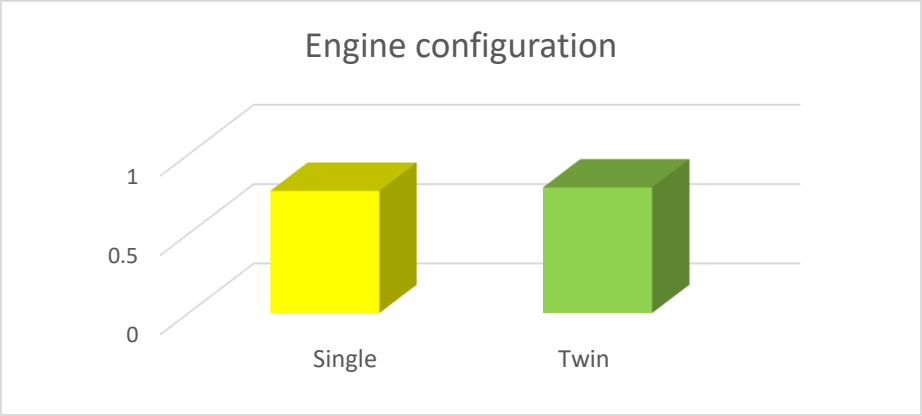

Figure 2.8 - Engine Configuration Trade Study

2.1.5 Landing Gear Type

Two different types of landing gear were compared. The first one is the tricycle landing gear that has a single nose wheel in the front, and two main wheels positioned close to the centre of gravity. The other alternative is the bicycle landing gear, also known as "taildragger", which consists in a pair of wheels ahead the centre of gravity with an additional smaller wheel in the back of the plane.

By comparing the two solutions, it was deduced that the tricycle leads to a greater structural weight than the bicycle. However, the weight gap is not wide enough to consider this aspect as a key factor for choosing one upon the other.

From the manoeuvrability point of view, it was found that the tailwheel-type landing gear, forces the aircraft to have a lower pitch angle during landing. That implies a strong use of the elevators to ensure a correct manoeuvre. Moreover, the relative position of CG and main landing gear does not mitigate the effect of the momentum generated by the friction between wheels and runway. Therefore, the rudder needs to make the aircraft stable also once it has touched the ground. On the other hand, the tricycle landing gear lets the aircraft fly at a greater angle of attack during approach to the runway, reducing landing speed and making the landing manoeuvre safer. The tricycle is also more stable during landing especially in case of single-engine configuration, as it guarantees more support to nose's structure that carries the propeller and the engine.

The two-wheeled gear is aerodynamically convenient because the area exposed to the airflow is less than it is in the tricycle configuration.

The final number of passengers will not be significantly affected by one of the different configurations considered. However, the tricycle is more comfortable because it does not involve any inclination of the fuselage during ground operations, so it is easier to load/unload passengers.

In case of the bicycle landing gear, there is a greater inclination between the aircraft and the ground that implies a drag increment and it complicates the take-off manoeuvre. This condition stands until the aircraft is aligned with the runway. The bicycle landing gear is also preferable on grass airfield. On the other hand, the tricycle landing gear gives some advantages in terms of thrust during the take-off run because the thrust vector is parallel to the ground. That allows a greater acceleration to quickly reach lift-off speed. This alternative is most suitable for asphalted runways.

Table 2.9 - Landing Gear Configuration Trade Study

GEAR CONFIGURATION TRADE STUDY					
		BICYCLE		TRICYCLE	
Attribute	Weighting	Insert Score	Weighted Score	Insert Score	Weighted Score
Structural Weight	16%	1	0.16	0.8	0.128
Manoeuvrability	12%	0	0	0	0
Passengers Capability	20%	0	0	0	0
Speed	14%	1	0.140	0.95	0.133
Manufacturability	18%	0	0	0	0
Take-Off Run	10%	0.7	0.070	1	0.100
Reliability	10%	0.5	0.050	1	0.100
Totals	100%		0.42		0.46

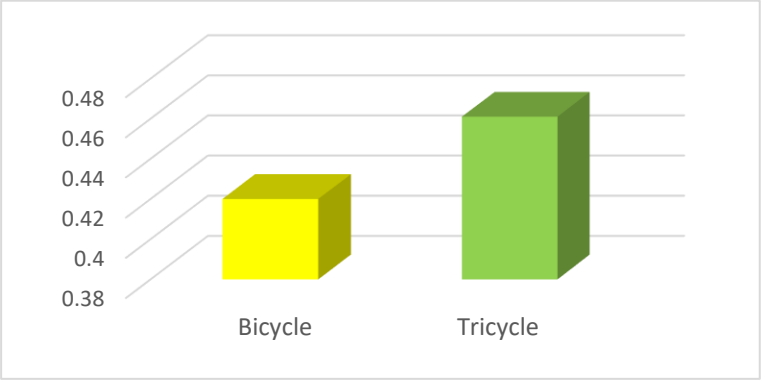

Figure 2.9 - Landing Gear Configuration Trade Study

2.1.6 Fuselage

The key factor for the analysis of the fuselage is the amount of payload it can carry. The types of fuselage taken into account are:

- CLASSIC: lobe structure which allows to define a practical shell structure involving curved plated beams and fuselage former.
- SMOOTHED RECTANGULAR: rectangular structure characterised by several corners that allow the structure itself to absorb greater loads. This phenomenon, however, means that in those points there is a greater probability of cracks propagation.

The smoothed rectangular section has a greater ease of construction and a better exploitability (more usable volume for a given section area) than the circular section.

Table 2.10 - Fuselage Configuration Trade Study

FUSELAGE SECTION CONFIGURATION TRADE STUDY					
		SMOOTHED RECTANGULAR		CIRCULAR	
Attribute	Weighting	Insert Score	Weighted Score	Insert Score	Weighted Score
Structural Weight	16%	1	0.16	1	0.16
Manoeuvrability	12%	0	0	0	0
Passengers Capability	20%	1	0.200	0.75	0.150
Speed	14%	0.75	0.105	1	0.140
Manufacturability	18%	1	0.180	0.4	0.072
Take-Off Run	10%	0	0	0	0
Reliability	10%	1	0.100	0.75	0.075
Totals	100%		0.745		0.597

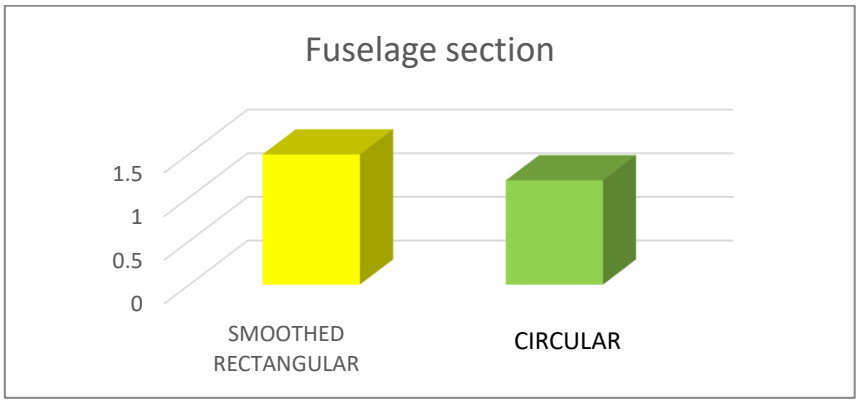

Figure 2.10 - Fuselage Configuration Trade Study

2.2 Sizing Process

Estimating dimensions and weights of the aircraft is a crucial phase of the design process and it allows the team to develop more detailed analysis based on aerodynamics, structures, and flight performance. The sizing process consists in an iterative procedure which starts giving as input the wing load *W/S* (statistically set), a plausible take-off and landing lift coefficient and the distance of the take-off run according to the requirements. The process ends when the variation of the final weight assumes a value within the 3% compared to the previous iteration.

Before calculating the weights, the determination of the power loading $\frac{W}{\Pi}$, where W is the max take-off weight and Π is the engine max power, is essential. First of all, the stall speeds during landing and take-off are easily calculable knowing the density of the air, the wing load, and the two lift coefficients $C_{L_{max_L}}$ and $C_{L_{max_{TO}}}$.

After that, according to the constraint about the take-off distance, it is possible to establish the thrust-to-weight ratio by using the simplified formula of the take-off run as it follows:

$$S_G = \frac{1.21\ W/S}{\rho g C_{L_{max_{TO}}}\ T/W} \quad \rightarrow \quad \frac{T}{W} = \frac{1.21\ W/S}{\rho g C_{L_{max_{TO}}} S_G}$$

Since the aircraft is propeller-driven, the power instead of the thrust has been considered during calculations. A proper approximation in take-off conditions is:

$$T = \frac{\Pi \eta_p}{0.7 \cdot 1.21 V_{S_{TO}}}$$

Furthermore, assuming a propeller efficiency value η_p relatively low (between 0.5 and 0.6), the following relation has been considered:

$$\frac{\Pi}{W} = \frac{0.7 \cdot 1.21^2\ W/S\ V_{S_{TO}}}{\eta_p \rho g C_{L_{max_{TO}}} S_G}$$

2.2.1 Weight Estimation

The characteristic weights of the aircraft are estimated in the following way.

The total weight (W) is given by the sum of different parts: structure, payload, engine (including prop), batteries and electronic parts. Passengers and their luggage constitute the payload to carry. They are respectively represented by standard cylinders and parallelepipeds made of wood. Their single weight is established by the requirements.

$$W = W_{\text{struct}} + W_{\text{payload}} + W_{\text{engine}} + W_{\text{batteries}} + W_{\text{electronic pts.}}$$

The structure's weight can be expressed by the following relation which takes into account the weight of the different structural components:

$$W_{\text{struct}} = W_{\text{wing}} + W_{\text{fuselage}} + W_{\text{h-tail}} + W_{\text{v-tail}} + W_{\text{gear}}$$

It is possible to statistically determine these weights by considering other aircraft with similar manufacturing characteristics (i.e. aircraft made of balsa wood). Then it is possible to evaluate for each component the weight to area ratio $W_{\text{comp}}/S_{\text{ref}}$ where S_{ref} is a characteristic surface of the component itself. That surface will be represented by the planform area for the wing and by the product of diameter and length for the fuselage (or eventually only for the length of the part with a constant cross section). The landing gear data can be obtained from statistics or relating it to the total weight. The $S_{\text{h-tail}}$ is considered as the 20-30% of the S_{wing}

$$\frac{W_{\text{wing}}}{S_{\text{wing}}} \quad \frac{W_{\text{fuselage}}}{D_{\text{fuselage}} L_{\text{fuselage}}} \quad \frac{W_{\text{h-tail}}}{S_{\text{h-tail}}} \quad \frac{W_{\text{v-tail}}}{S_{\text{v-tail}}} \quad \frac{W_{\text{gear}}}{S_{\text{gear}}} \quad \left(\text{or } \frac{W_{\text{gear}}}{W}\right)$$

The structure weight relation can be then developed by using these ratios as it follows:

$$W_{\text{struct}} = \frac{W_{\text{wing}}}{S_{\text{wing}}} S_{\text{wing}} + \frac{W_{\text{fuselage}}}{S_{\text{fuselage}}} S_{\text{fuselage}} + \frac{W_{\text{h-tail}}}{S_{\text{h-tail}}} S_{\text{h-tail}} + \frac{W_{\text{v-tail}}}{S_{\text{v-tail}}} S_{\text{v-tail}} + \frac{W_{\text{gear}}}{S_{\text{gear}}} S_{\text{gear}}$$

An iterative process is necessary as the surfaces considered before are initially unknown. Firstly, the areas values are assumed, then the weights of the single components are estimated as well as the total weight. Thus, the wing surface and the engine's weight can be determined by using the wing load and the power load previously obtained. The process explained is repeated until the difference between two consecutive iterations is less than 10 g.

It is assumed a wingspan of 5 ft by referring to the constraints given by the requirements and a value for the aspect ratio (i.e. AR = 8). It is also considered a rectangular wing because of its ease of manufacturing and its cost benefits:

$$AR = \frac{b^2}{S} \quad \Rightarrow \quad S = \frac{b^2}{AR}$$

$$S = bc \quad \Rightarrow \quad c = \frac{S}{b}$$

At this point, it is necessary to check whether the chord's length obtained is realistic comparing it to the fuselage one. While length and diameter of the fuselage depend on the payload, the tail and nose lengths are statistically determined by considering the ones of similar aircraft.

As the structure weight is now known, the weight of electronic parts, engines and batteries needs to be defined. This is possible by using catalogues on the internet that associates the maximum power supplied by the engine to its weight and to recommended electronic parts, such as ESC and batteries. The following ratios can be then determined assuming an initial power of 300-600 W:

$$\frac{W_{engine}}{\Pi} \quad \frac{W_{\text{batteries}}}{\Pi} \quad \frac{W_{\text{electronic pts.}}}{\Pi}$$

LEGEND	
Input Data	
Iterations results	

Table 2.11 - Iterations

ITERATIONS									
		ITERATION N. 1		ITERATION N.2		ITERATION N.3		ITERATION N.4	
Name	**Symbol**	**Quantity**	**Unit**	**Quantity**	**Unit**	**Quantity**	**Unit**	**Quantity**	**Unit**
Power needed	Π_n	150.77	W	152.46	W	152.92	W	153.04	W
ENGINE SYSTEM WEIGHT CALCULATION									
Engine weight	W_{engine}	0.044	Kg	0.045	Kg	0.045	Kg	0.045	Kg
Battery weight	$W_{battery}$	0.108	Kg	0.109	Kg	0.109	Kg	0.109	Kg
ESC weight	W_{ESC}	0.016	Kg	0.016	Kg	0.016	Kg	0.016	Kg
Engine Syst. weight	$W_{engine.pts.}$	0.168	Kg	0.170	Kg	0.171	Kg	0.171	Kg
STRUCTURAL WEIGHT CALCULATION									
Wing surface	S_{wing}	0.292	m^2	0.296	m^2	0.296	m^2	0.297	m^2
Fuselage diameter	D_{fus}	0.130	m	0.130	m	0.130	m	0.130	m
Fuselage length	L_{fus}	0.738	m	0.738	m	0.738	m	0.738	m
Horizontal tail surface	S_{H_tail}	0.058	m^2	0.059	m^2	0.059	m^2	0.059	m^2
Vertical tail surface	S_{V_tail}	0.020	m^2	0.021	m^2	0.021	m^2	0.021	m^2
Structural weight estimate	W_{struct}	1.417	Kg	1.424	Kg	1.426	Kg	1.426	Kg
Payload weight	$W_{payload}$	1.371	Kg	1.371	Kg	1.371	Kg	1.371	Kg
Total aircraft weight	W_{tot}	2.956	Kg	2.965	Kg	2.967	Kg	2.968	Kg
CHECK Chord	c	0.195	m	0.197	m	0.198	m	0.198	m
Weight variation	ΔW	0.033	Kg	0.009	Kg	0.002	Kg	0.001	Kg

PAYLOAD INPUT			
Name	**Symbol**	**Quantity**	**Unit**
Number of passengers	n	8	
Number of passengers for each row	N	2	
Passenger's length	a	0.031	m
Passenger's width	c	0.031	m
Passenger's height	l	0.09	m
Passenger's weight	M	113.4	g
Luggage length	a	0.019	m
Luggage width	c	0.025	m
Luggage height	l	0.038	m
Luggage weight	M	58	g

Table 2.13 – Payload Data Input

AIRCRAFT DATA INPUT			
Name	**Symbol**	**Quantity**	**Unit**
Wing Load	W/S	10	Kg/m^2
		98	N/m^2
Maximum landing lift coefficient	$CL_{max\_landing}$	1.8	
Maximum take-off lift coefficient	$CL_{max\_takeoff}$	1.5	
Take-off run	S_g	7.0	m
Wingspan	b	1.5	m
Aspect Ratio	AR	8.0	

Table 2.12 - Aircraft Data Input

DESIGN			
Name	**Symbol**	**Quantity**	**Unit**
Stall speed - Landing	$V_{stall\_landing}$	3.0	m/s
Rate Thrust - Weight	T/W	0.0959	N/kg
Stall speed – Take-off	V_{stall_TO}	3.3	m/s
Rate Power-Weight	Π/W	5.257	W/N
	Π/W	51.57	W/Kg
Structural Weight + Payload Weight	$W_{struct+payload}$	2.764	Kg
Structural Weight	W_{struct}	1.393	Kg
Payload Weight	$W_{payload}$	1.371	Kg
Power Required	Π_n	142.6	W
Electronics Weight	W_{elect}	0.159	Kg
Total Starting Weight	W_{tot}	2.923	Kg

Table 2.14 - Design Data

PAYLOAD STRUCTURE INFORMATION			
Name	**Symbol**	**Quantity**	**Unit**
Number of rows	N	4	
Passenger and Luggage seat length	a1	0.060	m
Passenger and luggage seat width	c1	0.037	m
Passenger and luggage height	H	0.108	m
Total length of payload grid	A	0.240	m
Total width of payload grid	C	0.074	m
Final length of payload grid	A_{final}	0.264	m
Final width of payload grid	C_{final}	0.081	m
Front part length	r	0.204	m
Tail length	j	0.270	m
Aircraft Length	L	0.738	m
Payload Weight	$W_{payload}$	1371.2	g

Table 2.15 - Payload Structure Information

STATISTIC ESTIMATION			
STRUCTURAL WEIGHT ESTIMATION			
RATIOS ESTIMATION			
Name	**Symbol**	**Quantity**	**Unit**
Wing's ratio	W_{wing}/S_{wing}	1.83	Kg/m^2
Fuselage's ratio	$W_{fus}/(D_{fus}\cdot L_{fus})$	8.30	Kg/m^2
Horizontal tailplane's ratio	W_{H_tail}/S_{H_tail}	1.06	Kg/m^2
Vertical tailplane's ratio	W_{V_tail}/S_{V_tail}	1.25	Kg/m^2
WEIGHTS ESTIMATION			
Name	**Symbol**	**Quantity**	**Unit**
Wing surface	S_{wing}	0.2813	m^2
Fuselage diameter	D_{fus}	0.1296	m
Fuselage length	L_{fus}	0.7383	m
Horizontal tailplane surface	S_{H_tail}	0.0563	m^2
Vertical tailplane surface	S_{V_tail}	0.0197	m^2
Structural Weight	W_{struct}	1.393	Kg

Table 2.16 - Weight Estimation

Considering the final values of weight regarding the electronics, the team selected real components that very closely match the ones coming from our model. Regarding the single engine configuration, the propulsion will be offered by the "A20-22L EVO kv924" from *Hacker* with the paired ESC "X-12-Pro". For the twin engine configuration, instead, the most suitable engine is "A20-30M EVO kv980". The battery that will power the propulsive system will be a "20C-ECO-X 1450mAh 3S-slim" from *TopFuel*.

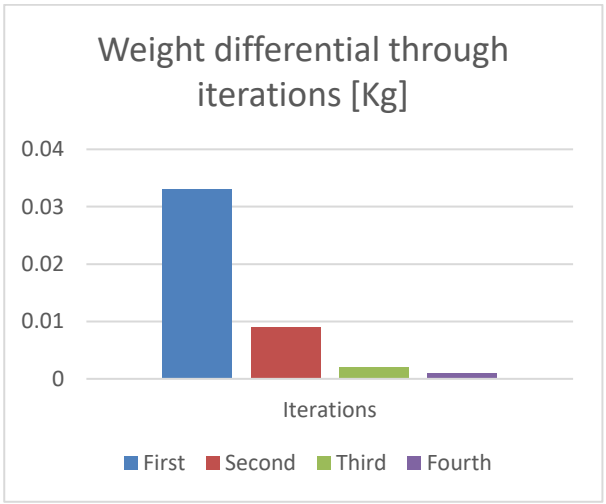

Figure 2.11 - Weight Differential through iterations

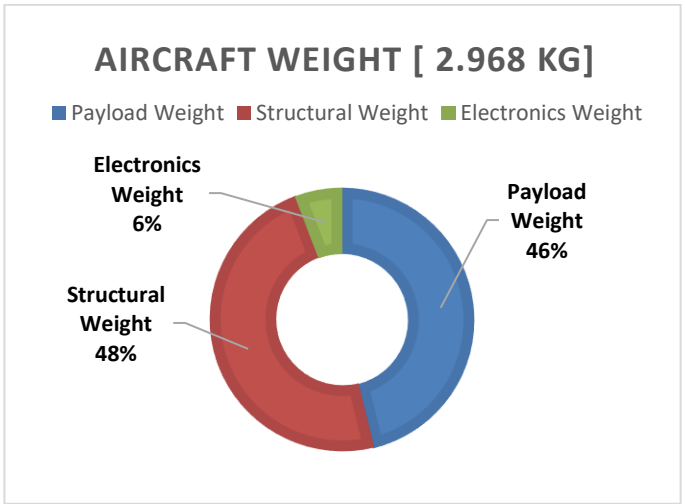

Figure 2.12 - Aircraft Weight

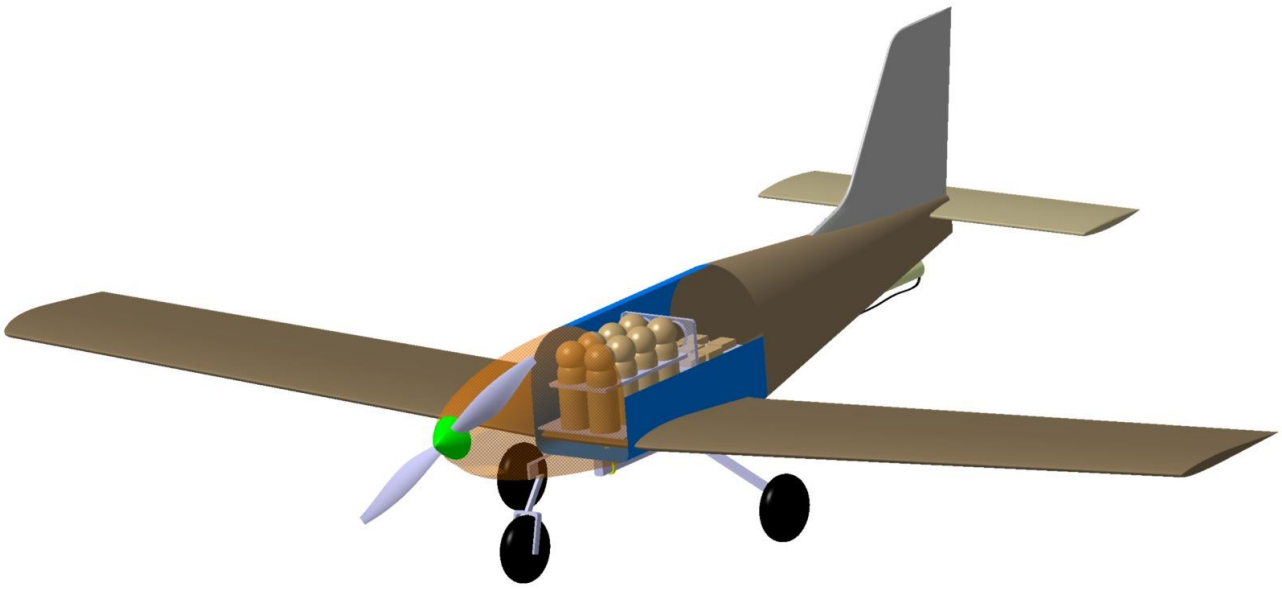

Figure 2.13 - First Aircraft Sketch (single engine configuration)

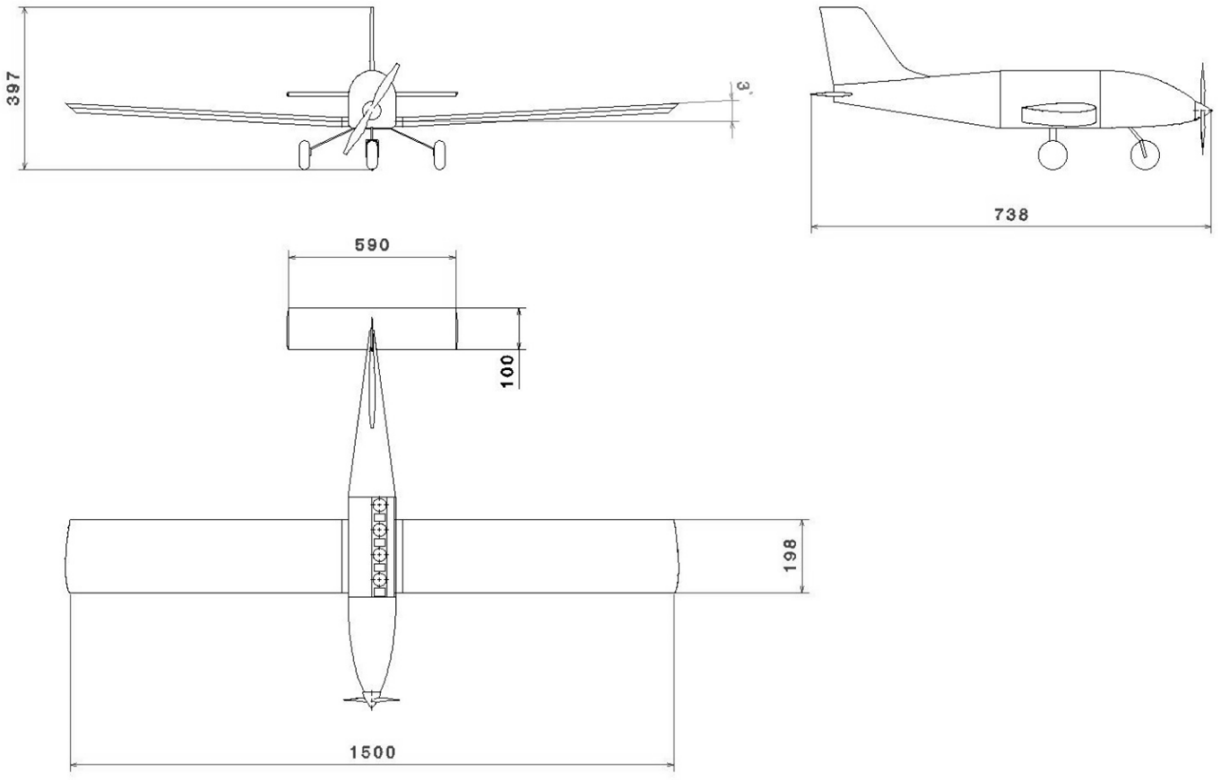

Figure 2.14 - Aircraft Three Views

Chapter 3

Aerodynamics

3. Introduction

The aim of this section is to study the aerodynamics of the wing of the aircraft as well as to evaluate the influence of a towed banner in terms of additional drag. In particular, the aerodynamic configuration has been analyzed and designed using XFOIL and XFLR5 which are software developed for the design and the analysis of subsonic airfoils as well as for the stability study.

3.1 Airfoil selection

The choice of a suitable airfoil is crucial to allow the aircraft to fulfil the required flight performance. As a consequence, several airfoils have been considered. All the airfoils were analyzed at different Reynolds numbers in order to predict some aerodynamic parameters in all flight conditions.

First of all, the sought airfoil must allow sufficient lift to carry as much payload as required being able to have good performance at low Reynolds numbers. This means also to have as little drag as possible, therefore, a high lift/drag ratio is required for an efficient cruise. Moreover, for succeeding in a short take-off, the airfoil should guarantee a high $C_{L_{max}}$ without flaps (at least 1.4).

Secondly, in order to accommodate spars, wing-internal mounted servos, and other internal structures, the airfoil should have a minimum thickness of 10% of the chord length.
In addition, low thickness airfoils often have abrupt stall characteristics at low angles of attack that would hinder the pilot during the flight.

Finally, a flat bottom airfoil is preferred to ensure an easy and reliable manufacturing. For the same reason, high camber airfoils are avoided because it may turn out to be tricky at shaping highly curved surfaces with balsa wood. Furthermore, although they would provide high cruising speed, they would require greater thrust on take-off which could be not supplied during the take-off run.

The airfoils taken into consideration are E-221, NACA 4412, CLARK Y and FX 63-137 and are shown below.

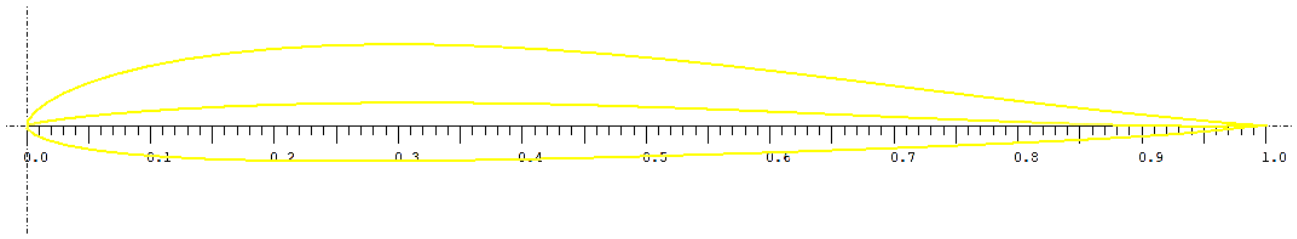

Figure 3.15 - EPPLER-221

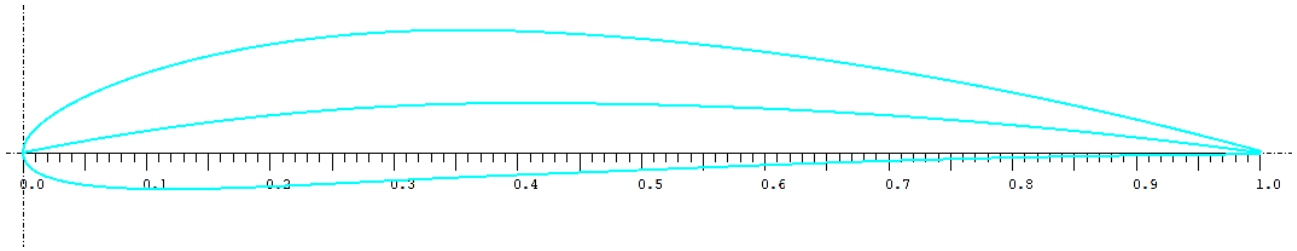

Figure 3.16 - NACA 4412

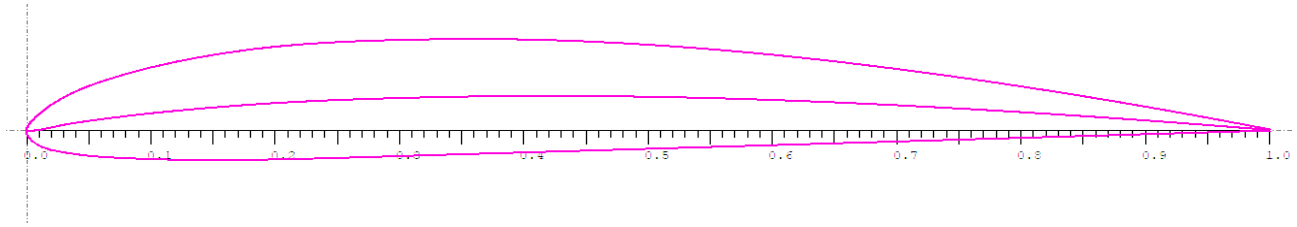

Figure 3.17 - CLARK Y

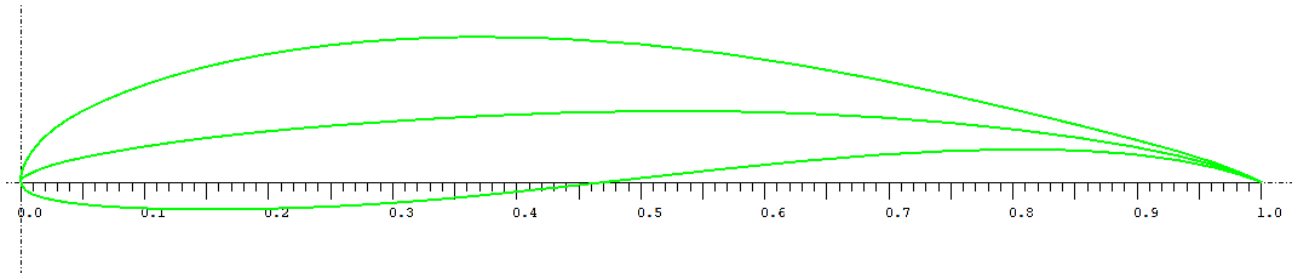

Figure 3.18 - WORTMANN FX 63-137

The following table includes the main geometric properties of the four airfoils.

Table 3.17 - Geometry Comparison

Geometric Parameter	E-221	NACA 4412	CLARK Y	FX 63-137
Max. Thickness [%]	9.4	12	11.7	13.7
Max. Thickness at Chord Lenght [%]	28.1	30	28	30.9
Max. Chamber [%]	1.6	4	3.4	6
Max. Chamber at Chord Lenght [%]	32.6	40	42	53.3

Information for the airfoils has been obtained from the *UIUC Airfoil Database*[1] and they have been compared using XFLR5[2], which is a translation of the FORTRAN program XFOIL[3], developed by Dr. Mark Drela from MIT. The comparison between the airfoils has been made at the expected range of Reynolds number from 150.000 to 300.000 at Mach 0. In particular, the most explanatory graphs are in order: C_l vs α, C_l vs C_d, C_d vs α, C_m vs α and C_l/C_d vs α, where C_l, C_d and C_m are respectively the non-dimensional coefficients of lift, drag, and pitching moment.

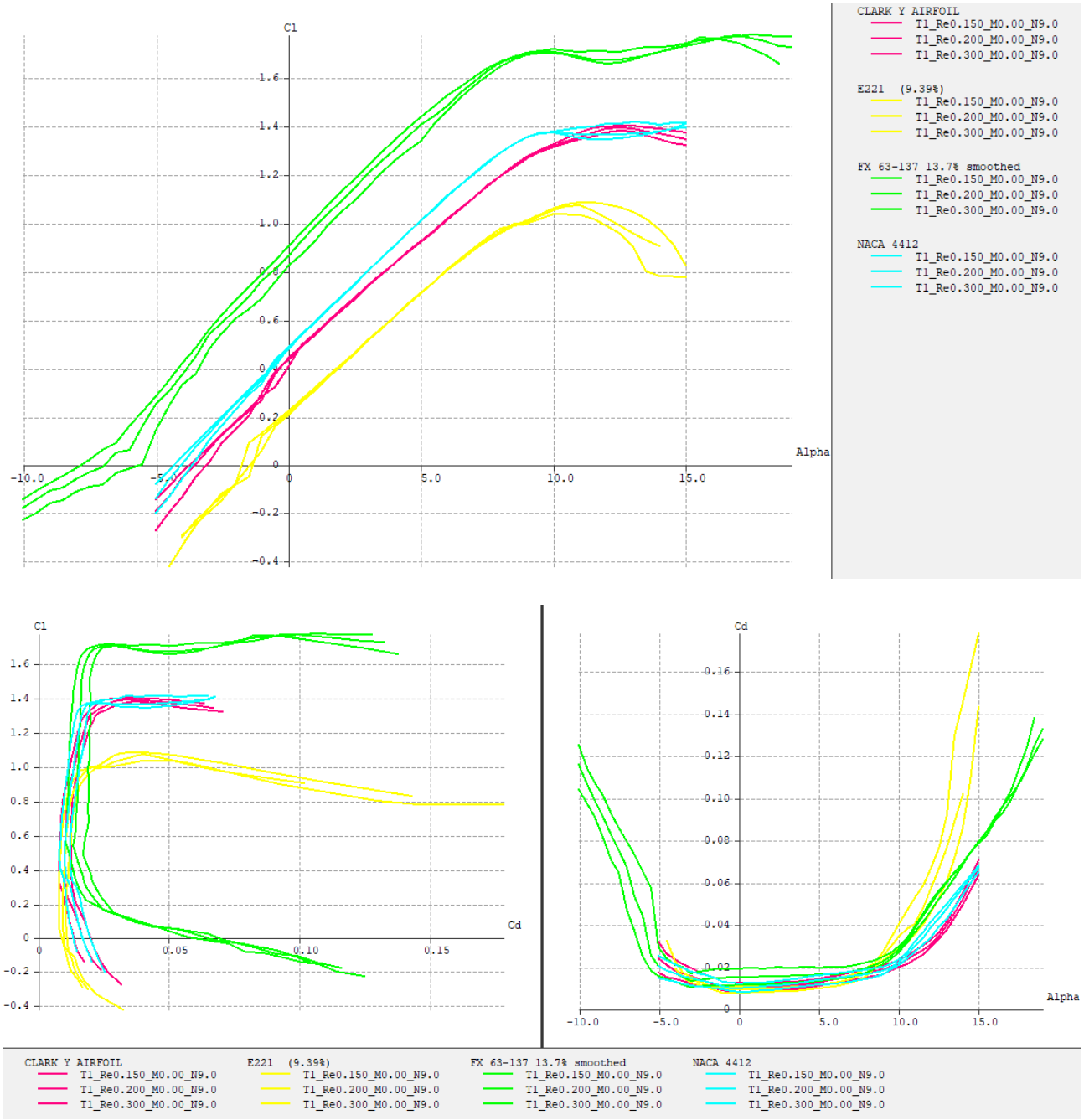

Figure 3.19 - C_l vs α, C_l vs C_d and C_d vs α graphs

[1] https://m-selig.ae.illinois.edu/ads/coord_database.html
[2] http://www.xflr5.tech/
[3] https://web.mit.edu/drela/Public/web/xfoil/

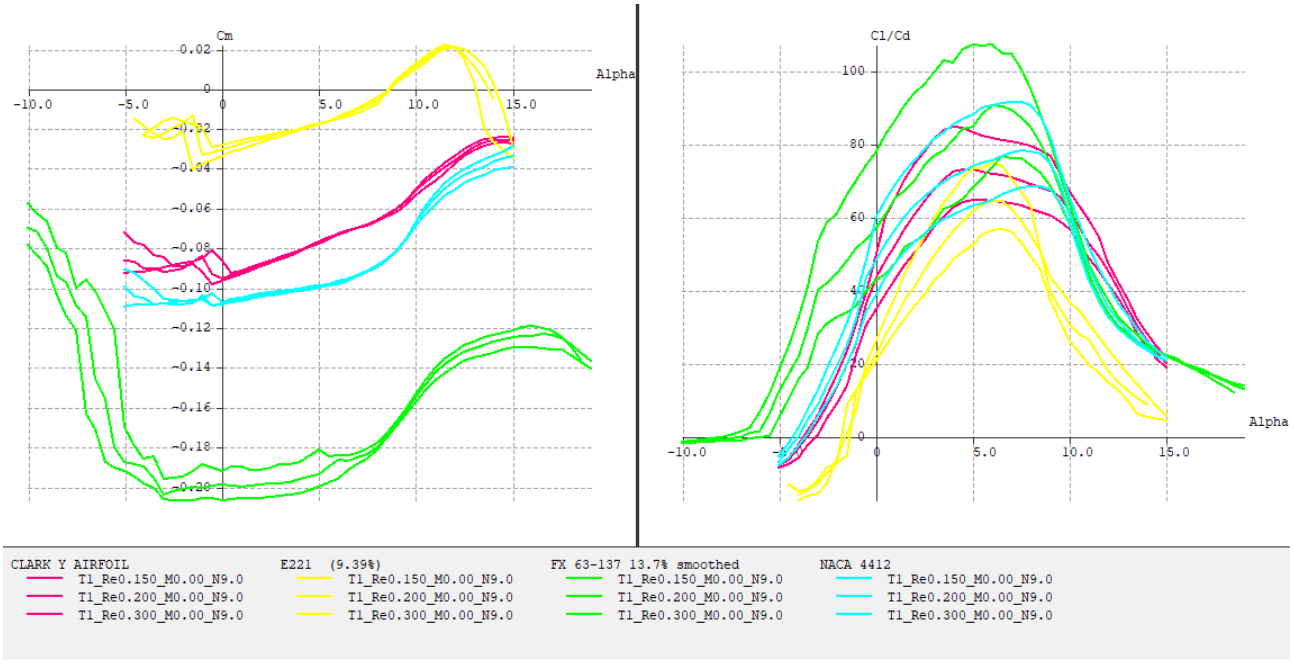

Figure 3.20 - C_m vs α and C_l/C_d vs α graphs

The five graphs imply that the best airfoil is the Wortmann FX 63-137 mainly in terms of aerodynamic efficiency and high lift coefficient with equal angle of attack. Nevertheless, its complex geometry is extremely difficult to manufacture. Indeed, its high curvature and sharp trailing edge do not allow an easy manufacture and they might cause imperfection in the balsa wood surfaces of the airfoil. Also, it has a zero-lift pitching moment coefficient which is twice the value achieved with a NACA airfoil. As a result, both the airfoil performance and aircraft stability could be compromised.

The NACA 4412 and CLARK Y have almost the same characteristics. Both of them provide a properly $C_{l_{max}}$ and efficiency. Furthermore, the drag coefficient stays low for a wide range of lift coefficients. However, the flatter bottom of the CLARK Y airfoil is preferred in manufacture-wise. As shown in the graphs, the EPPLER-221 airfoil has the lower aerodynamics performance especially as far as $C_{l_{max}}$ is concerned, which is mostly important to pursue a short take-off run.

The ensuing table contains the main aerodynamics parameters obtained from the software analysis in order to have another direct comparison of the airfoils.

Table 3.18 - Main Aerodynamics Parameters

Main Aerodynamics Parameters	E-221	NACA 4412	CLARK Y	FX 63-137
$C_{l\,0}$	0.224	0.478	0.436	0.882
$C_{l\,max}$	1.034	1.409	1.380	1.763
$C_{l\,\alpha}$ [rad^{-1}]	6.28	6.28	6.28	6.28
$C_{d\,0}$	0.011	0.012	0.013	0.019
$C_{m1/4}$	-0.034	-0.108	-0.096	-0.192

For all these reasons, the airfoil selected is CLARK Y. It is the most suitable also taking manufacturability into consideration. In fact, this airfoil has a relatively low maximum camber of 3.4%, a taper trailing edge and thickness achievable from balsa wood construction. In addition, a maximum thickness of 11.7% assures the successful accommodation of the wing's internals.

Regarding the tailplane, the airfoil chosen for the horizontal stabilizer is the NACA 0009 whereas for the vertical stabilizer the best choice is likely to be the Selig S9026.

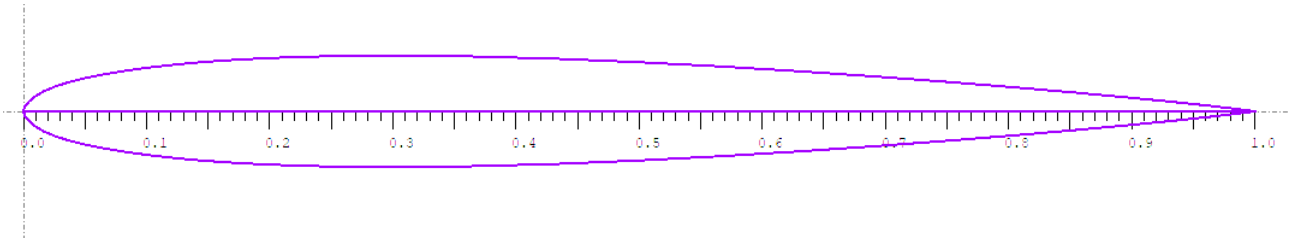

Figure 3.21 - NACA 0009

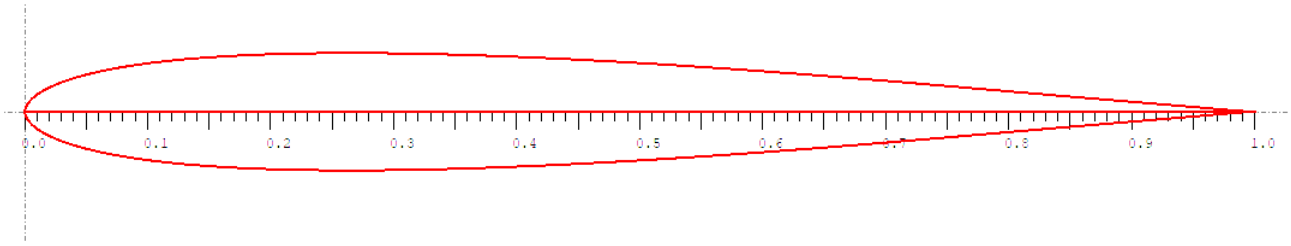

Figure 3.22 - SELIG S9026

3.2 Airfoil Analysis

The CLARK Y airfoil has been analyzed at different numbers of Reynolds and in a range of angle of attack from -5° to 15°. The distribution of the coefficient of pressure C_p along the chord is showed below for three different angles of attack.

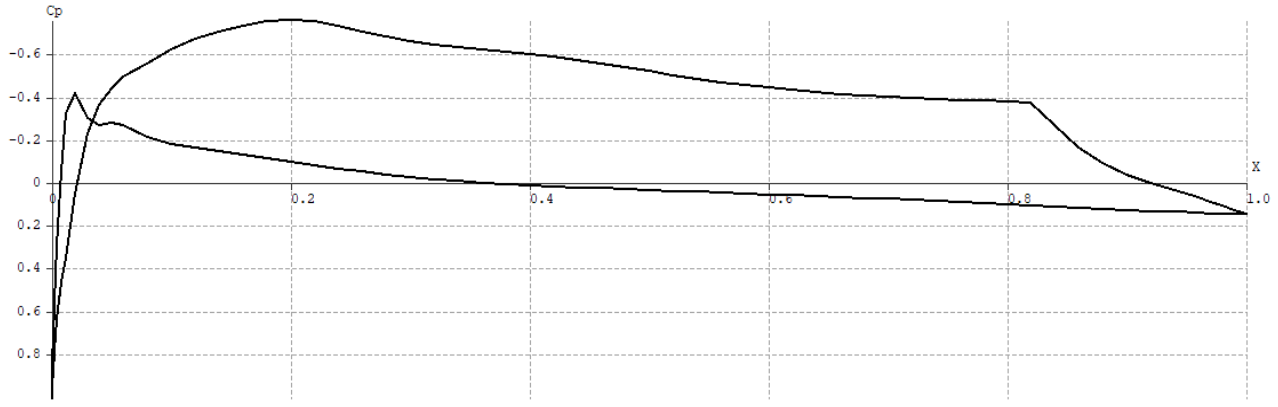

AoA 0°

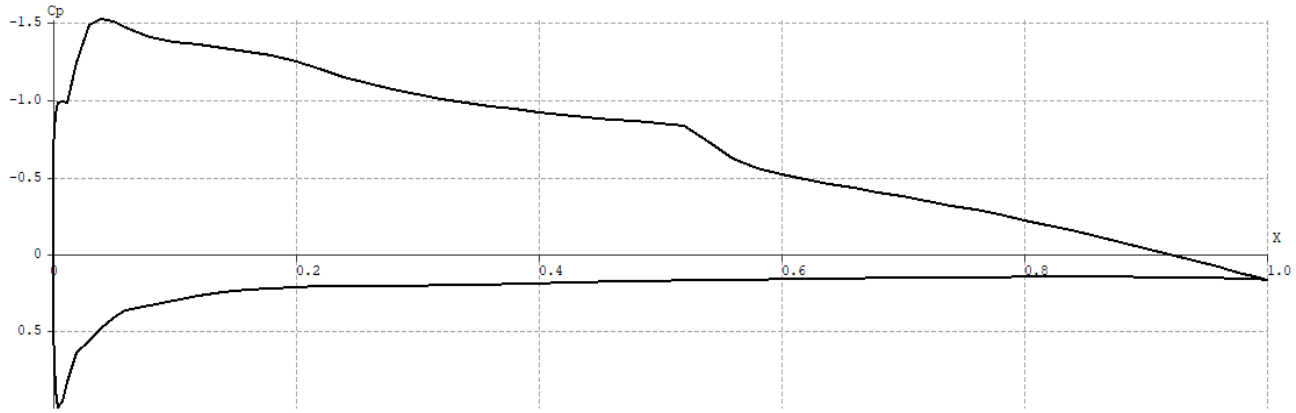

AoA 5°

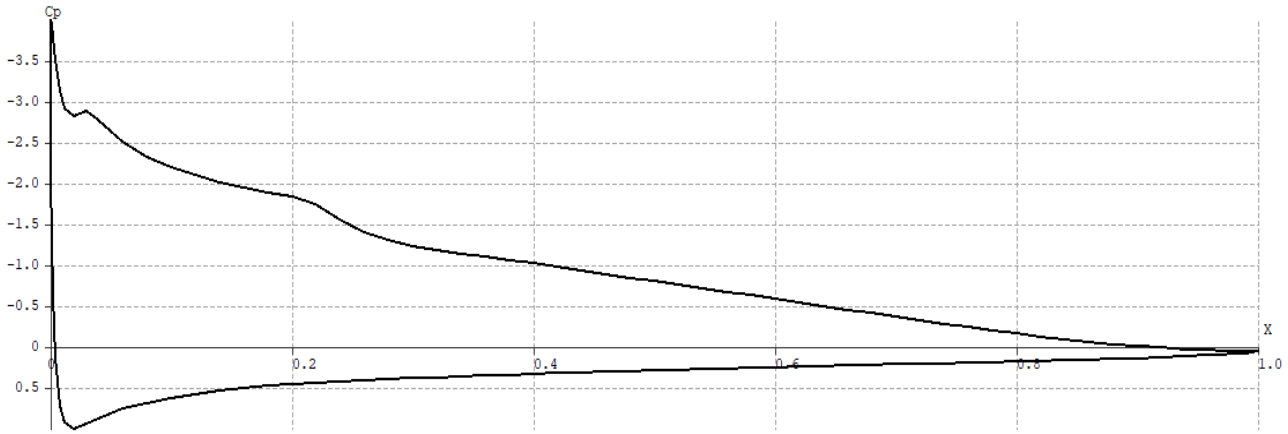

AoA 10°

Figure 3.23 - C_p graphs

3.3 Wing Analysis

Once the airfoil had been selected, the aircraft's wing has been modeled using XFLR5's wing and plane analysis section. This dedicated section of the software exploits the vortex lattice method (VLM) to model the surfaces as thin planes of discrete ring and horseshoe vortices in order to compute the lift and induced drag.

According to the preliminary sizing, the wing of the aircraft is rectangular with a span of 1,5 m and 0,198 m of chord. Moreover, it is assumed a 3° dihedral angle and no tapering or twisting. The total mass considered of the aircraft is 2,968 kg.

The modeled wing is shown below with the representation of the lift (green lines), the viscous drag (violet lines) and the downwash (red lines). As previously, the analysis has been made for three different angles of attack at the cruise speed.

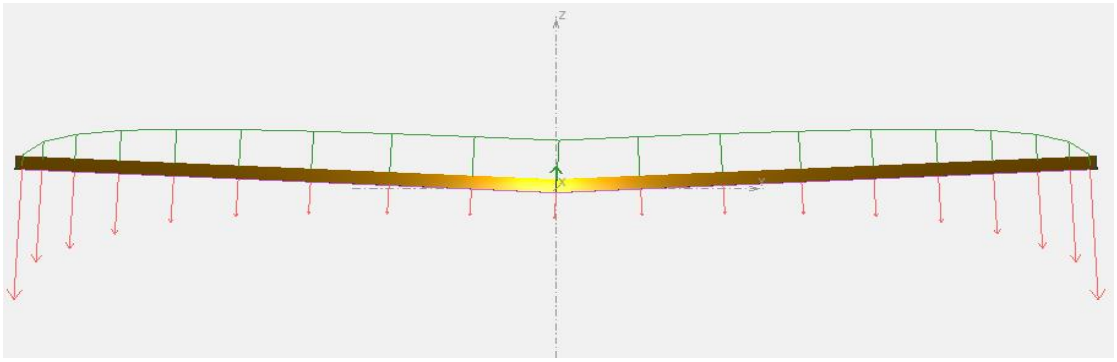

Figure 3.24 - Front view

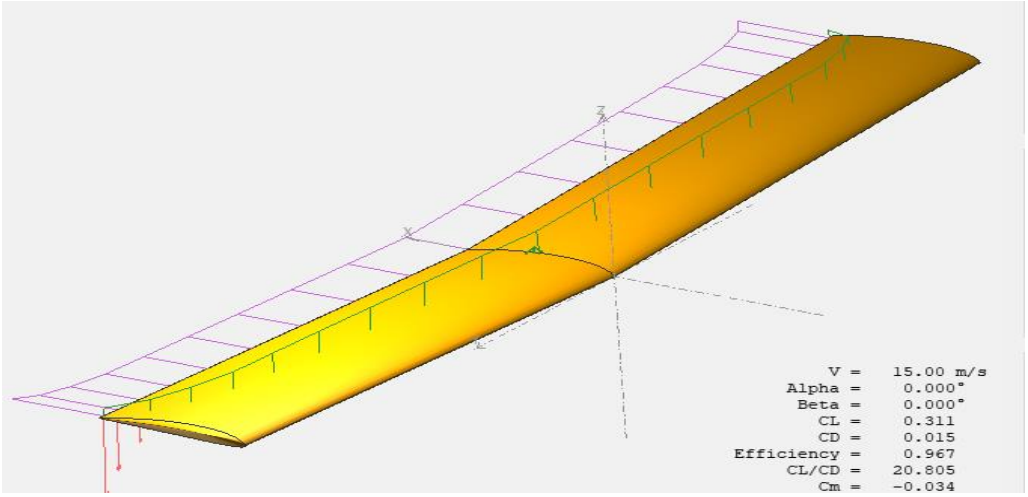

AoA 0°

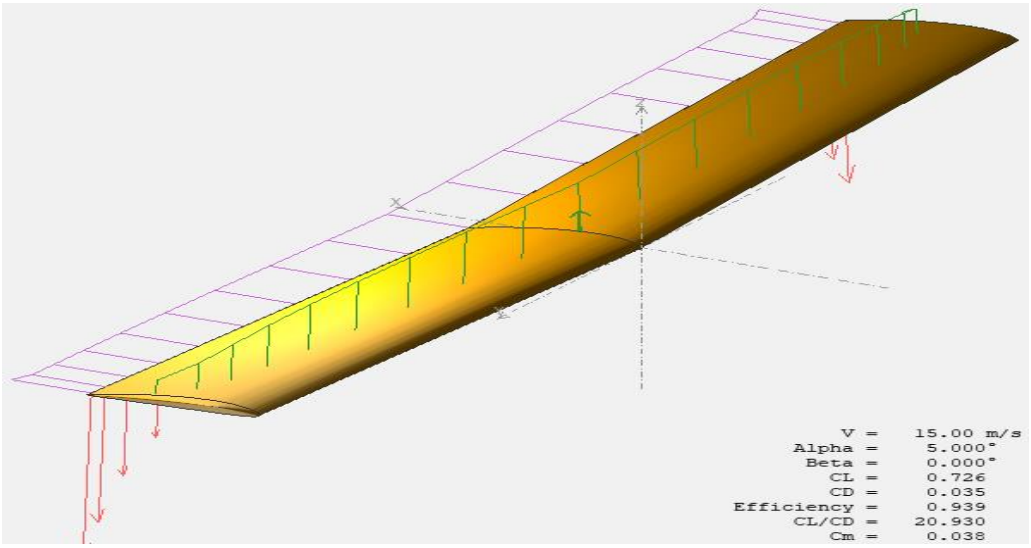

AoA 5°

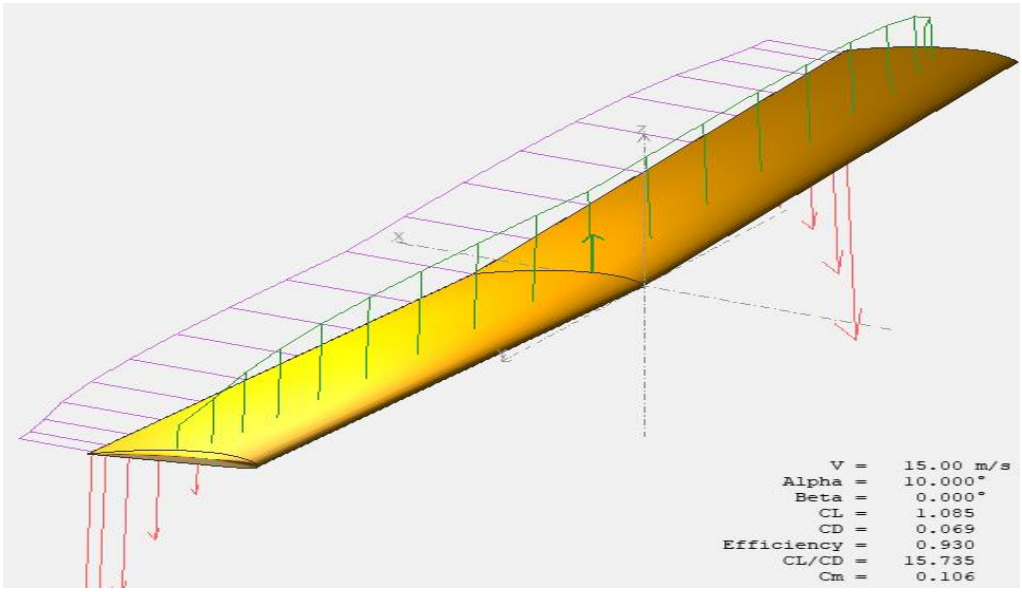

AoA 10°

Figure 3.25 - Wing Analysis

Furthermore, the wing has been analyzed for three different air speeds, obtaining the following graphs. The clean wing stalls at $C_L = 1{,}2$ at 5 m/s and at $C_L = 1{,}3$ at higher speeds, which are acceptable values for the expected performance[4].

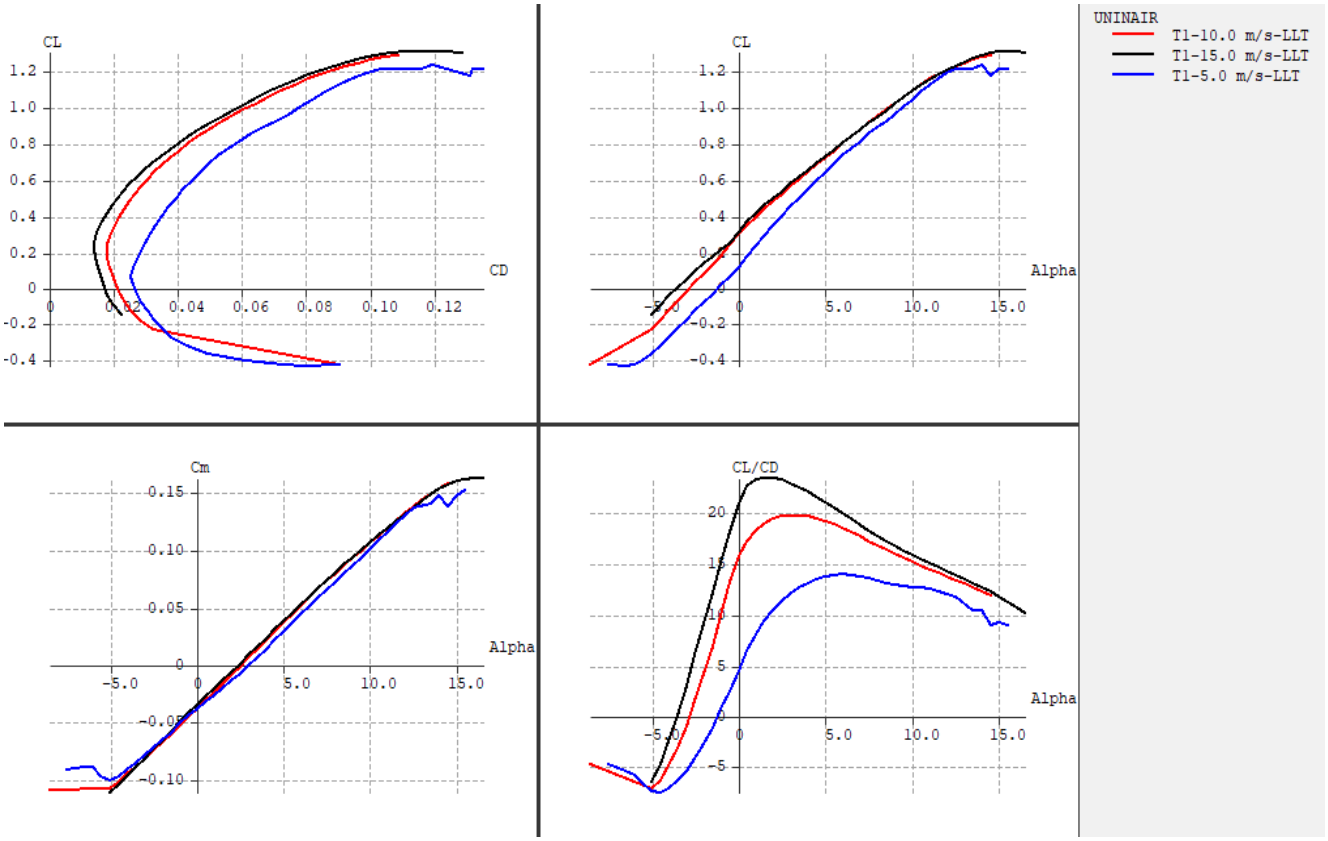

Figure 3.26 - Final Wing's analysis graphs

[4] See the thesis of Francesco Granata - Preliminary Sizing and Flight Performance of a Single-Electric Powered RC Aircraft, 2020.

3.4 Banner

This paragraph is intended to evaluate the additional drag caused by the deployment of a banner in a range of known dimensions. This study is due to the necessity of predicting the behavior of a banner towing plane to avoid abrupt and uncontrolled maneuvers during the mission.

It is considered a rectangular banner of lawn hooked into the rear part of the aircraft.
The total drag coefficients, drag at 100 ft/sec, weight and fineness ratio of the flags are given in Table 3.19.

Table 3.19 - Banner's Parameters

Drag of Flags of Different Shape, Density and Fineness Ratio.

Rectangular.									
Fineness ratio	2·0	1·5	1·0	0·75	0·5	0·48	0·25	1·0	0·97
Weight per sq. ft. ω	0·016	0·016	0·016	—	—	0·016	—	0·0075	0·032
Span s (ft.)	4	4	4	—	—	4	—	9·5	1·875
Density ratio $\sigma = \frac{\omega}{s\rho g}$	0·0523	0·0523	0·0523	—	—	0·0523	—	0·0103	0·223
Drag at 100 ft./sec. (lb.)	15·0	14·3	12·4	—	—	10·4	—	34·0	9·0
k_D	0·020	0·025	0·033	—	—	0·057	—	0·016	0·11
$\frac{k_D - 0·012}{\sigma}$	0·153	0·248	0·401	—	—	0·860	—	0·388	0·439
Triangular.									
Weight per sq. ft. ω	—	—	0·016	0·016	0·016	—	0·016	—	—
Span s (ft.)	—	—	4	4	4	—	4	—	—
Density ratio σ	—	—	0·0523	0·0523	0·0523	—	0·0523	—	—
Drag at 100 ft./sec. (lb.)	—	—	12·9	11·7	10·8	—	8·8	—	—
k_D	—	—	0·034	0·041	0·057	—	0·095	—	—
$\frac{k_D - 0·012}{\sigma}$	—	—	0·421	0·554	0·861	—	0·586	—	—

After several experiments, it was proved that the measured drag coefficients were practically independent of Reynolds number [R.A. Fairthorne, 1930]. Therefore, for all flags of given geometrical type, the drag coefficient k_D may be taken to be the sum of a function of two variables, fineness ratio and density ratio, and the other a function of the viscous forces, i.e. the skin friction. The value of the skin friction coefficient C_f has been taken empirically as 0.012.

The Density Ratio is $\sigma = \frac{w}{s\rho g}$ where w is the weight per unit area of the flag, s the span, ρ the volume density of the air and g is the acceleration due to gravity.

The Fineness Ratio is defined as the area of the banner divided by the square of the span.

The esteem of the additional drag is made considering the drag coefficient based on unit projected area. It is obtained from the following diagram where is plotted the k_D coefficient changing the fineness ratio. As shown, for different banners with the same span and weight per area unit, the drag coefficient increases with the reduction of the area of the flag.

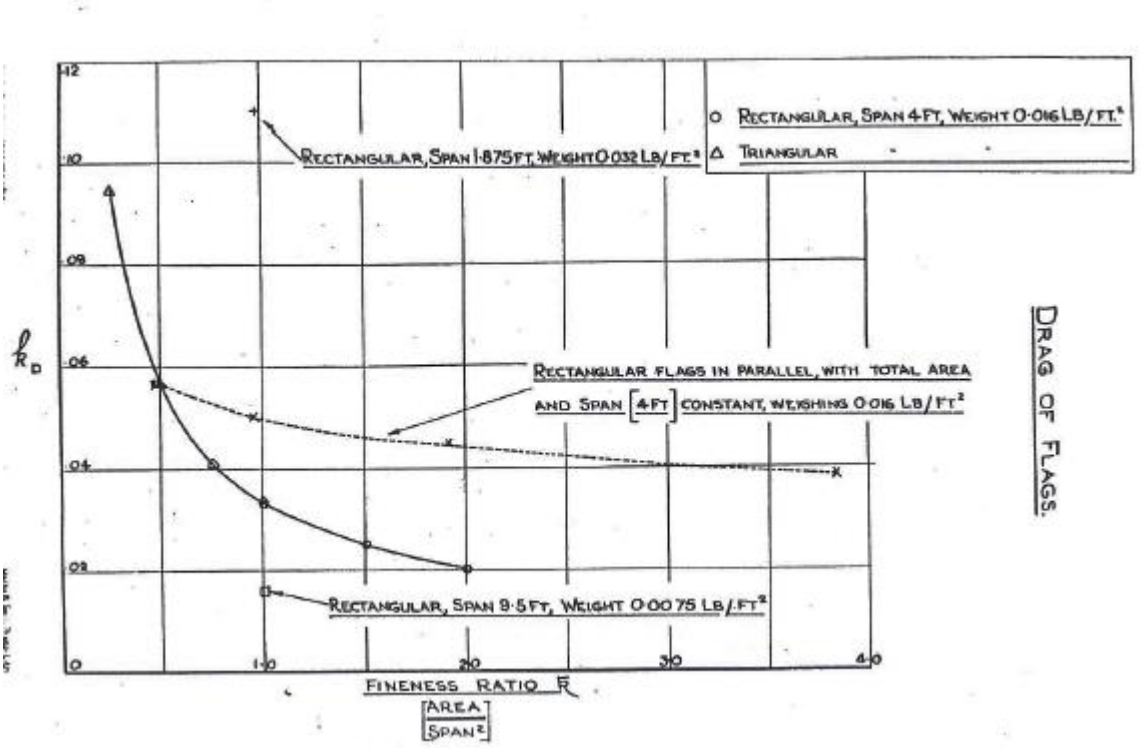

Figure 3.27 - Banner's k_D graph

For instance, it is calculated the extra drag coefficient of a rectangular banner whose dimensions are 10 inches of length and 5 inches of height.

Since the calculated area is 50 square inches, the fineness ratio is calculated as follows:

$$Fineness\ Ratio = \frac{Area}{Span^2} = 0.5$$

As a result, the estimated drag coefficient is $k_D \cong 0.0570$ on the banner area. This value is scaled by the ratio of banner area over wing area to be added to the aircraft drag coefficient

$$\Delta C_D = k_D \frac{S_{\text{banner}}}{S_{\text{wing}}} = 0.0061$$

where $S_{\text{banner}} = 50\ in^2 = 0.032\ m^2$ and $S_{\text{wing}} = 0.297\ m^2$. The additional drag coefficient due to the installation of a 10 by 5 inches (about 25 by 13 cm) banner, neglecting the support system, is 61 drag counts.

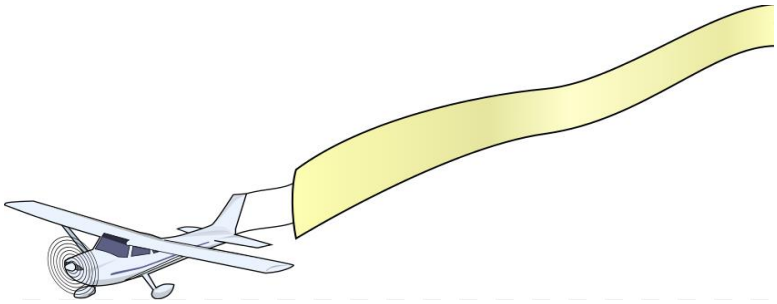

Figure 3.28 - Banner Towing Plane

Chapter 4

Propeller choice

4. Introduction

To provide the required thrust and power to the aircraft is important in order to guarantee good flight performances for different flight conditions and reasonable consumptions during the mission. Therefore, the choice of the propeller is a fundamental step of the whole project.
A variety of propellers has been compared using the available data from *UIUC Propeller Data Site*[5]. The analysis has been made for both the configurations introduced previously, in static condition or at cruise speed.

4.1 Twin engine configuration

The total power estimated with the sizing process is about 153 W. From *Hacker Brushless Motors* website[6], the selected engine is "A20-30M EVO kv980".

Figure 4.29 - Twin-engine configuration's motor

According to the motor's specifications (3S with a voltage of 3.7 V per cell), the maximum number of RPM is about 10900. Nevertheless, it is considered the 70% of the nominal value that is about 7900 so that there is an extra power exploitable in emergency case.

The propeller chosen for the twin engine configuration is *APC thin electric 9x6* (9-inch diameter propeller with a pitch of 6 inch/revolution). All the relevant values obtained from the graphs available from the database, have been collected in the table below.

[5] https://m-selig.ae.illinois.edu/props/propDB.html
[6] https://www.hacker-motor-shop.com/brushless-motors.htm?shop=hacker_e&SessionId=&a=catalog&p=3

Table 4.20 - Twin-engine's propeller data

				APC Electric 9X6						
Diameter [m]	n [s^{-1}]	J	C_{P0}	C_{T0}	P_0	T_0	C_P	C_T	P	T
0,229	132	0,496	0,05	0,11	88,72 W	6,46 N	0,045	0,08	79,85 W	4,69 N

J is the advance ratio calculated as $J = \frac{V}{nD}$ where V is the cruise speed (approximately $15\ m/s$), n represents the number of revolutions per sec and D is the diameter of the propeller. The coefficients C_T and C_P are the Renard coefficients determined as follows:

$$C_T = \frac{T}{\rho n^2 D^4}\ ;\ C_P = \frac{P}{\rho n^3 D^5}$$

P is the power and T is the thrust, both calculated with the inverse formula. The subscript 0 is referred to the static case. The static thrust is grater because the propeller compresses the air more efficiently at lower speeds.

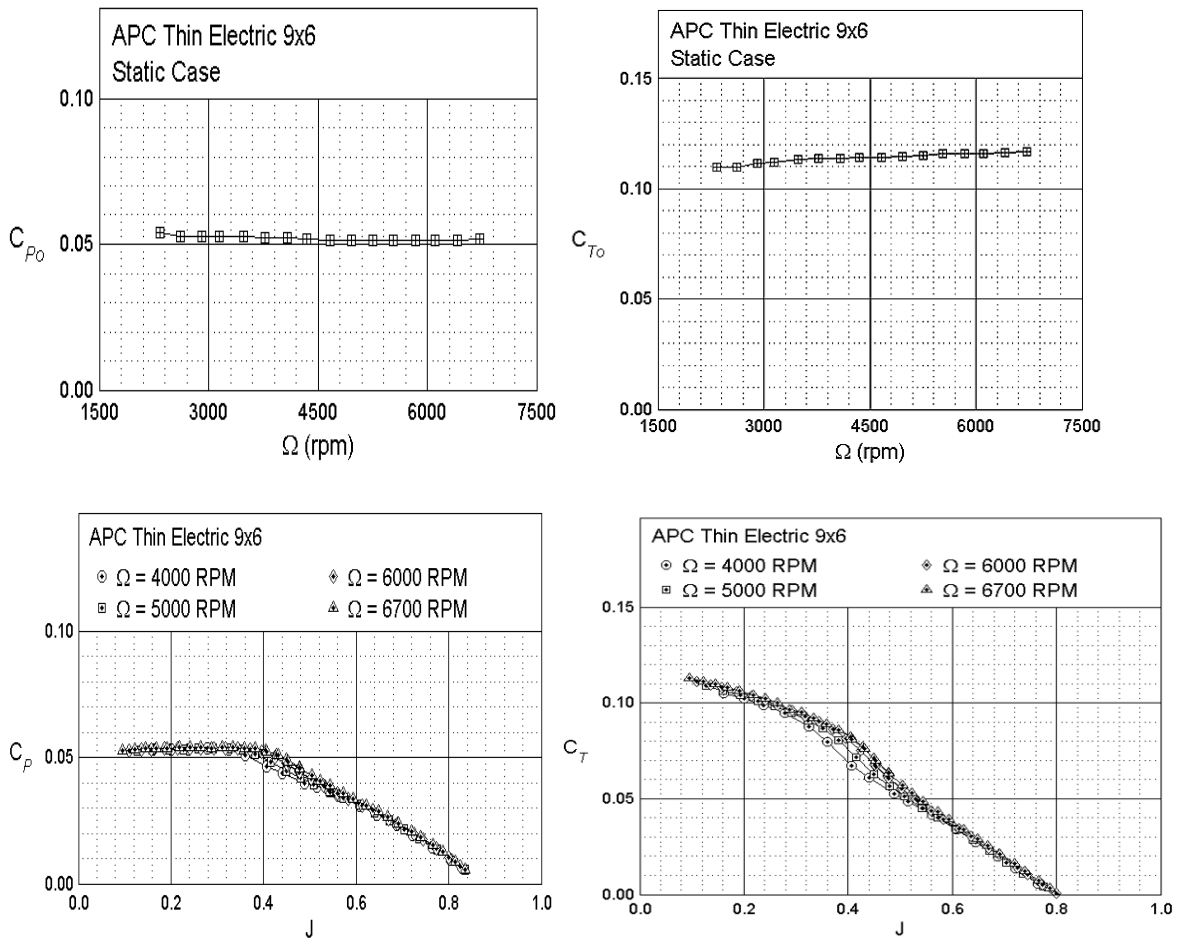

Figure 4.30 - APC Thin Electric 9x6 graphs

As far as the efficiency is concerned, there is just a maximum value because the propeller is fixed pitch. For the value of J obtained previously, the analyzed propeller has $\eta = 0.67$.

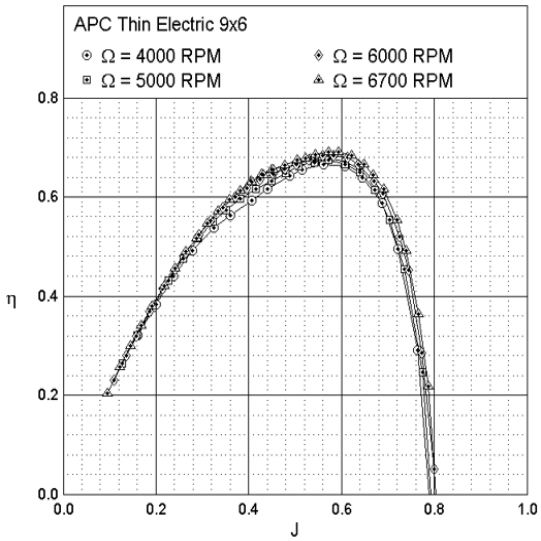

Figure 4.31 - Twin-engine's propeller efficiency

4.2 Single engine configuration

Regarding the single engine configuration, the most suitable propeller is *APC thin electric 11x7* (11-inch diameter propeller with a pitch of 7 inch/revolution). Since the clearance is greater, for this configuration a propeller with a greater diameter has been selected in order to provide a higher value of the thrust. As previously, the propeller performances have been evaluated at fixed point as well as at cruise speed.

The single engine selected for this configuration from *Hacker Brushless Motors* website is the "A20-22L EVO kv924".

Figure 4.32 - Single engine configuration's motor

Also, according to the motor's specifications, the RPM value is about 7230 (i.e. 121 s^{-1}). In this case, the values obtained from the graphs are the followings:

Table 4.21 - Single engine's propeller data

				APC Electric 11X7						
Diameter [m]	n [s^{-1}]	J	C_{P0}	C_{T0}	P_0	T_0	C_P	C_T	P	T
0,28	121	0,443	0,043	0,11	160,60 W	12,13 N	0,042	0,085	156,87 W	9,37 N

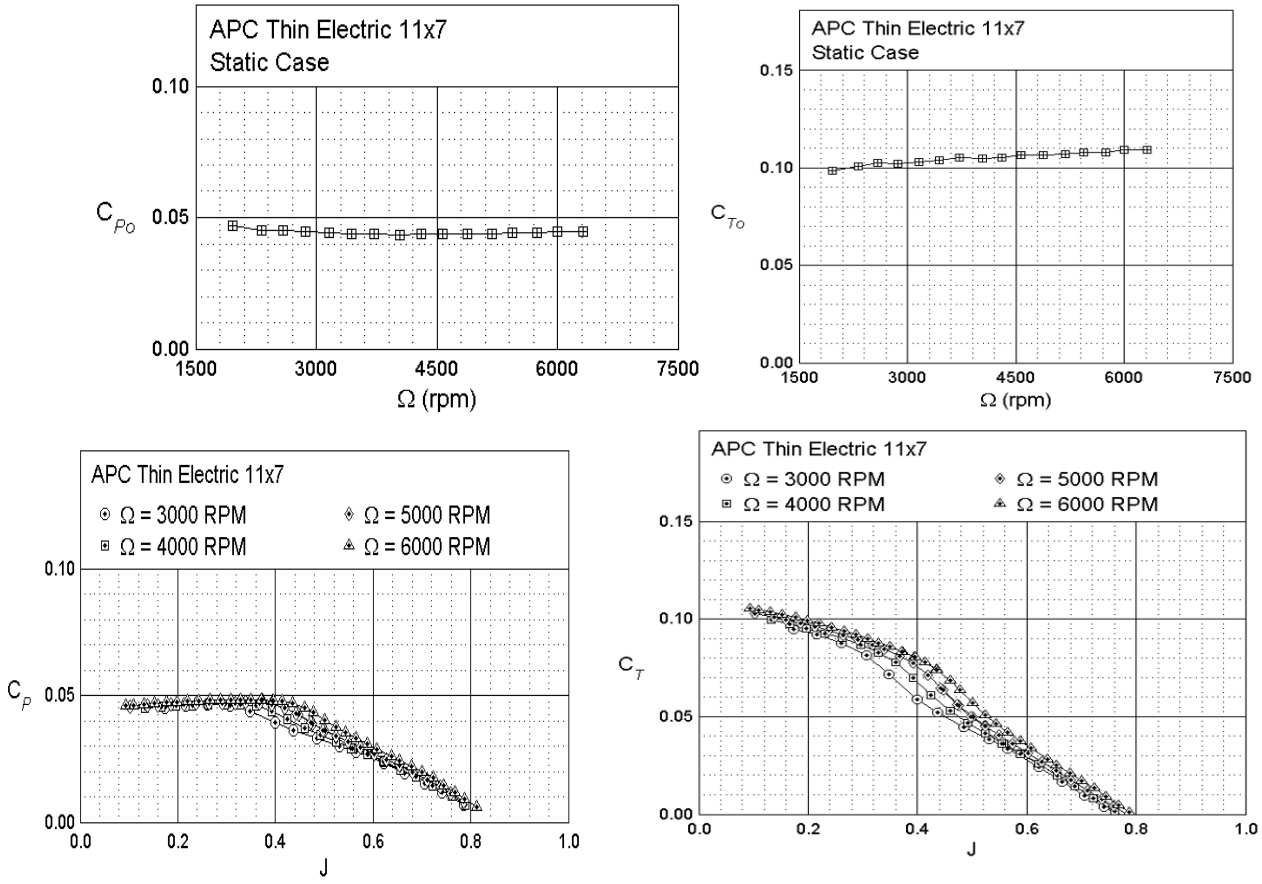

Figure 4.33 - APC Thin Electric 11x7 graphs

From the ensuing graph, it is obtained that the efficiency value is about $\eta = 0.7$.

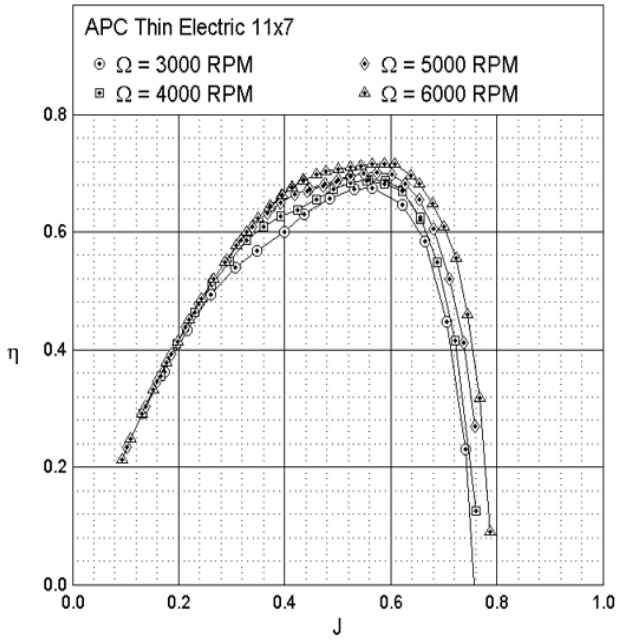

Figure 4.34 - Single engine's propeller efficiency

Bibliography

[1] Martin Simons, “Model Aircraft Aerodynamics”, Argus Books, 1978.

[2] Special Convention RAA News. Regional horizons. RAA Annual Convention, Milwaukee, Wisconsin, May 2010.

[3] Bombardier Aerospace Commercial Aircraft Market Forecast. Commercial aircraft market forecast 2012-2031. 2012. URL: http://www2.bombardier.com/en/3_0/3_8/market_forecast.

[4] Simpson, R., Junction flows. Annual Review of Fluid Mechanics, 33, 2001.

[5] Hoerner, S. F., Fluid dynamic drag. Horner Fluid Dynamics, 1965.

[6] Schlichting, H., Truckenbrodt, E., A., “Aerodynamic of the Airplane”, 1st ed., McGraw-Hill, USA, 1979, Chaps 5, 6.

[7] Siegel, S., Comparison of design rules regarding the wing-body junction flow of a subsonic aircraft. University of Technology Dresden, Department of Aerodynamics, 30 June 2011.

[8] Jacobs E. and Ward, K., Interference of wing and fuselage from tests of 209 combinations in the NACA variable-density test tunnel. NACA Technical Report No. 540, 1935.

[9] Muttray,H., Aerodynamic aspects of wing-fuselage fillets. NACA Technical Memorandum No.764, 1935.

[10] Fleming, J., Simpson, R., Cowling, J. and Devenport, W., An experimental study of a turbulent wing-body junction and wake flow. Experiments in Fluids, 14, 1993.

[11] Oelcmen, S. and Simpson, R., Some structural features of a turbulent wing-body junction vortical flow. Report No. VPI-AOE-238, Virginia Polytechnic Institute and State University Blackburg, 1996.

[12] Boermans, L., M., M. and Nicolosi, F., “Sailplane fuselage and Wing-Fuselage junction design,” XXV Ostiv Congress, S. Auban France, 3-11 July 1997.

[13] Boermans, L. M. M., Nicolosi, F. and Kubrynski, K., Aerodynamic design of high performance sailplane wing fuselage combinations. 21st ICAS Conference, Paper No.A98-31523(ISBN-10:1-56347-287-2), 13 -18 September 1998.

[14] White, J. A. and Hood, M. J., Wing-fuselage interference tail buffeting and air flow about the tail of a low wing monoplatet, NACA Technical Report No.482, 1933.

[15] Maughmer,M., Hallmann,D., Ruszkowski, R., Chappel, G. and Waitz, I, Experimental investigations of wing-fuselage integration geometries, AIAA Journal of Aircraft, 26(8), 1989.

[16] R.A. Fairthorne, Drag of Flags. Reports and Memoranda No.1345, May, 1930.